HHS Public Access

Author manuscript

Sci Immunol. Author manuscript; available in PMC 2017 August 16.

Published in final edited form as:

Sci Immunol. 2017 May 19; 2(11): . doi:10.1126/sciimmunol.aal1713.

Intratumoral delivery of inactivated modified vaccinia virus Ankara (iMVA) induces systemic antitumor immunity via STING and Batf3-dependent dendritic cells

Peihong Dai[1,2,#], **Weiyi Wang**[1,#], **Ning Yang**[1], **Cristian Serna-Tamayo**[1], **Jacob M. Ricca**[3], **Dmitriy Zamarin**[3,4,5,6], **Stewart Shuman**[2], **Taha Merghoub**[3,4,5], **Jedd D. Wolchok**[3,4,5,6], and **Liang Deng**[1,6,*]

[1]Dermatology Service, Department of Medicine, Memorial Sloan Kettering Cancer Center, New York, NY 10065

[2]Molecular Biology Program, Memorial Sloan Kettering Cancer Center, New York, NY 10065

[3]Parker Institute for Cancer Immunotherapy, Memorial Sloan Kettering Cancer Center, New York, NY 10065

[4]Ludwig Center for Cancer Immunotherapy, Memorial Sloan Kettering Cancer Center, New York, NY 10065

[5]Melanoma and Immunotherapeutics Service, Department of Medicine, Memorial Sloan Kettering Cancer Center, New York, NY 10065

[6]Weill Cornell Medical and Graduate Colleges, New York, NY 10065

Abstract

Advanced cancers remain a therapeutic challenge despite recent progress in targeted therapy and immunotherapy. Novel approaches are needed to alter the tumor immune-suppressive microenvironment and to facilitate the recognition of tumor antigens that leads to antitumor immunity. Poxviruses, such as modified vaccinia virus Ankara (MVA), have potential as immunotherapeutic agents. Here we show that infection of conventional dendritic cells (DCs) with heat-inactivated or UV-inactivated MVA leads to higher levels of IFN induction than MVA alone through the cGAS–STING cytosolic DNA-sensing pathway. Intratumoral injection of inactivated MVA (iMVA) was effective and generated adaptive antitumor immunity in murine melanoma and

[*]corresponding author. Mailing address for Liang Deng: Dermatology Service, Department of Medicine, Memorial Sloan Kettering Cancer Center, 1275 York Ave., New York, NY 10065. dengl@mskcc.org.

[#]These two authors contributed equally to this work.

Author contributions: L.D. designed and performed the experiments, analyzed the data, and prepared the manuscript. P.D., W.W., and N. Y. performed the experiments, analyzed the data, and assisted in manuscript preparation. C.S.T., J.M.R. and D.Z. assisted in some experiments and data interpretation. S.S., T.M., J.D.W. assisted in experimental design, data interpretation, and manuscript preparation.

Competing interests: Memorial Sloan Kettering Cancer Center filed a patent application for the use of MVA and inactivated MVA as monotherapy or in combination with immune checkpoint blockade for solid tumors. L.D., P.D., W. W., N.Y., S.S., T.M., and J.D.W. are authors on the patent applications.

colon cancer models. iMVA-induced antitumor therapy was less effective in STING- or Batf3-deficient mice than in wild-type mice, indicating that both cytosolic DNA-sensing and Batf3-dependent $CD103^+/CD8\alpha^+$ DCs are essential for iMVA immunotherapy. The combination of intratumoral delivery of iMVA and systemic delivery of immune checkpoint blockade generated synergistic antitumor effects in bilateral tumor implantation models as well as in a unilateral large established tumor model. Our results suggest that inactivated vaccinia virus could be used as a immunotherapeutic agent for human cancers.

Introduction

Induction of host antitumor immunity contributes to the efficacy of virus-based oncolytic therapies (1–3). Therefore, the identification of relevant components of the innate and adaptive immune systems that are activated by virotherapy, and the design of optimal strategies to enhance antitumor immunity by engineering recombinant viruses, could lead to better treatment options for advanced cancers.

Type I interferons (IFN) play important roles in host antitumor immunity (4). IFNAR1-deficient mice are more susceptible to development of tumors after implantation of tumor cells compared with wild-type (WT) controls. Spontaneous tumor-specific T cell priming is also defective in IFNAR1-deficient mice (5, 6). Pathways linked to IFN production are mechanistically linked to tumor biology and therapy. The cytosolic DNA-sensing pathway is important in the innate immune sensing of tumor-derived DNA, which leads to the development of antitumor $CD8^+$ T cell immunity (7). DNA-sensing also plays an important role in radiation-induced antitumor immunity (8).

In this study, we investigated the use of non-replicative, heat- or UV-inactivated modified vaccinia virus Ankara (Heat-iMVA or UV-iMVA) as an immunotherapeutic agent in two murine cancer models: melanoma and colon cancer. MVA is a highly attenuated vaccinia strain that has been used as a vaccine vector against diverse infectious agents (9–13). Here, we provide evidence that intratumoral injection of inactivated MVA (iMVA) alters the tumor microenvironment in both injected and non-injected tumors and results in systemic antitumor immunity. These immunologic effects are dependent on STING-mediated cytosolic DNA-sensing and on Batf3-dependent $CD103^+/CD8\alpha^+$ dendritic cells (DCs).

Immune checkpoints have been implicated in the downregulation of anti-tumor immunity. Antibodies targeting immune checkpoint proteins or their ligands (CTLA-4, PD-1, or PD-L1) disinhibit anti-tumor T cells, leading to proliferation and survival of activated T cells, or reversal of T cell exhaustion (14–17). Despite the success of immune checkpoint blockade, not all patients respond and lack of baseline tumor immune infiltration is logically linked to absence of response. We found that intratumoral delivery of iMVA overcomes resistance to immune checkpoint blockade in murine tumor models. Our results suggest that iMVA is an effective immune-stimulating agent and the combination of intratumoral injection of iMVA and systemic delivery of immune checkpoint blockade may be adopted in clinical settings as strategy to improve treatment in malignancies that are refractory to checkpoint blockade.

Results

Heat-inactivated MVA induces higher levels of type I IFN production in murine cDCs than MVA

Infection of cDCs with MVA induces type I IFN via the cytosolic DNA sensor cGAS and its adaptor STING (18). We inferred that MVA encodes one or more proteins that attenuate the induction of type I IFN, in light of findings that infection of cDCs with MVAΔE3L (a mutant that lacks the gene encoding the poxvirus virulence factor E3) triggered the induction of higher levels of type I IFN than did MVA (18). We hypothesized that infection with inactivated MVA (iMVA) might also elicit an enhanced IFN response. Inactivation was achieved by heating MVA at 55°C for 1 h, which reduced infectivity by 1000-fold (19). Murine cDCs were infected in parallel with MVA (at a multiplicity of 10) or with an equivalent amount of Heat-iMVA. We found that Heat-iMVA infection induced higher levels of *Ifna4* and *Ifnb* mRNA than MVA (Fig. 1 A). Heat-iMVA-infected cDCs secreted higher levels of IFN-α and IFN-β than those induced by MVA (Fig. 1B). Western blot analysis showed that E3 protein (a viral early gene product) was not produced in Heat-iMVA-infected cDCs, but was expressed in MVA-infected cells (fig. S1A). Heat-iMVA triggered higher levels of IRF3 phosphorylation than MVA at 4 h and 8 h post-infection (fig. S1A). The effects of varying the temperature of the virus pre-treatment on the strength of the IFN response were gauged by infecting cDCs with equivalent amounts of virus that had been incubated for 1 h at 45, 50, 55, 60, or 65°C. MVA heated at 55°C induced the highest levels of IFN-α and IFN-β secretion (fig. S1B).

Innate immune response to Heat-iMVA depends on cytosolic DNA-sensing by cGAS/STING, transcription factors IRF3/IRF7, and IFNAR1

To test whether Heat-iMVA induction of type I IFN is mediated through the cGAS/STING pathway, we generated cDCs from cGAS$^{-/-}$ mice and age-matched wild-type (WT) controls, and infected them with Heat-iMVA. Induction of *Ifna4* and *Ifnb* mRNAs at 6 h post-infection was effaced in cGAS-deficient cells (Fig. 1C). ELISA of supernatants collected at 22 h post-infection also showed that Heat-iMVA-induced IFN-α/β secretion was abolished in cGAS-deficient cells (Fig. 1D). STING is a critical adaptor for the cytosolic DNA-sensing pathway (20–23). We generated cDCs from STING$^{Gt/Gt}$ mice that lack functional STING (18, 24) and found that Heat-iMVA-induced type I IFN gene expression and IFN-α/β secretion depended on STING (Fig. 1, E and F). Heat-iMVA infection caused phosphorylation of IRF3 at Ser-396 at 4 h and 8 h post-infection, which was absent in cGAS- or STING-deficient cells (fig. S1, C and D).

To test whether and how Heat-iMVA infection triggers DC maturation, we infected cDCs from STING$^{Gt/Gt}$ mice and age-matched WT controls with Heat-iMVA. Cells were collected at 14 h post-infection and stained for MHCI, CD40, CD86, and CD80. FACS analysis showed that Heat-iMVA infection induced the expression of MHCI, CD40, CD80, and CD86 in WT cells, which was only slightly elevated in STING-deficient cells (Fig. 1G, H). We conclude that Heat-iMVA induces DC maturation via the cytosolic DNA-sensing pathway.

Using cDCs derived from genetic knock-out mice, we found that Heat-iMVA-induced *Ifna4* and *Ifnb* gene expression and secretion of IFN-α and IFN-β proteins depended on transcription factors IRF3, IRF7 and the IFN receptor IFNAR1, but not on transcription factor IRF5 (fig. S1, E-H).

UV-inactivated MVA induces type I interferon in cDCs in a STING-dependent manner

Parallel experiments were performed with MVA that had been inactivated by irradiation with ultraviolet light (UV-iMVA). cDCs from $STING^{Gt/Gt}$ mice and WT controls were infected with MVA at a MOI of 10, or with an equivalent amount of Heat-iMVA, or UV-iMVA. Similar to Heat-iMVA, UV-iMVA induced higher levels of type I IFN than MVA in WT cDCs (fig. S2, A and B). UV-iMVA induction of type I IFN was abolished in STING-deficient cells (fig. S2, C and D) and UV-iMVA-induced phosphorylation of IRF3 was absent in $STING^{Gt/Gt}$ cells that had no detectable STING protein (fig. S2E).

Heat-iMVA infection of B16-F10 melanoma cells induces the production of type I IFN and proinflammatory cytokines and chemokines

To test whether Heat-iMVA infection of tumor cells also triggers innate immune responses, we infected B16-F10 melanoma cells with MVA at a MOI of 10, or with an equivalent amount of Heat-iMVA. Heat-iMVA infection induced higher levels of *Ifna4, Ifnb, Ccl5*, and *Il6* gene expression than MVA at 6 h post-infection (Fig. 2A). Heat-iMVA caused higher levels of IFN-α, IFN-β, CCL5, and IL-6 protein secretion from B16-F10 cells than MVA at 22 h post-infection (Fig. 2B). Heat-iMVA induced higher levels of phosphorylation of IRF3 in B16-F10 melanoma cells than MVA (Fig. 2C). Furthermore, Heat-iMVA infection induced the expression of MHC Class I on B16-F10 cells, whereas MVA infection did not (Fig. 2D). These results suggest that Heat-iMVA infection induces innate immune responses and promotes immunogenicity of the infected tumor cells.

PD-L1 expression on tumor cells is frequently up-regulated by type I IFN and IFN-γ. We found that Heat-iMVA infection of B16-F10 cells induced PD-L1 expression whereas MVA infection did not (fig. S3, A and B). The mean fluorescence intensity (MFI) of PD-L1 expression was increased by 4-fold in Heat-iMVA-infected cells compared with MVA-infected cells (fig. S3, A and B).

Heat-iMVA infection of human melanoma cells SK-MEL-146 (which has WT BRAF) also triggered type I IFN and inflammatory cytokine and chemokine production. We found that Heat-iMVA induced higher levels of Ifnb, Cxcl9, Cxcl10, Il-6, and Ccl4 gene expression than MVA. The fold-induction of *Ifnb*, Il6, *Ccl4, Cxcl9*, and *Cxcl10* gene expression by Heat-iMVA was 4172, 51, 6.9, 5792, and 932-fold respectively, compared with 192, 36, 4.4, 52, and 94-fold by MVA (fig. S4, A-F). These results indicate that Heat-iMVA is a stronger inducer of innate immunity than MVA in human melanoma cells. Heat-iMVA infection also induced PD-L1 expression on SK-MEL-146 cells. The MFI of pD-L1 expression was increased from 99 in MVA-infected cells to 217 in Heat-iMVA-infected cells (fig. S4, G and H).

Intratumoral injection of Heat-iMVA into implanted B16-F10 melanoma induces the production of type I IFN and proinflammatory cytokines and chemokines

To understand the innate immune response of tumor microenvironment to intratumoral injection of MVA or Heat-iMVA *in vivo*, we implanted B16-F10 melanoma cells intradermally. When the tumors were 5–6 mm in diameter, we injected either MVA (2 × 10 pfu), or an equivalent amount of Heat-iMVA or PBS twice with three days apart. Two days after the second injection, tumors were harvested and RNAs were extracted from tumor cells. Quantitative PCR analyses were performed and we found that intratumoral injection of Heat-iMVA induced higher levels of *Ifnb, Ccl4, Ccl5*, and *Cxcl10* gene expression than MVA in murine tumor microenvironment (Fig. 2E-H). These results indicate that Heat-iMVA is a stronger inducer of innate immunity than MVA in murine implanted tumors in vivo.

Intratumoral injection of Heat-iMVA leads to tumor eradication and durable systemic antitumor immunity in a murine transplantable B16-F10 melanoma model

We established a murine melanoma model through intradermal implantation of B16-F10 melanoma cells (1×10^5) on one side of the flank of C57B/6 mice. Ten days after tumor implantation, when the tumors were approximately 3 mm in diameter (the mean initial volumes for the PBS and Heat-iMVA groups are 24 mm^3 and 16 mm^3), we began injecting Heat-iMVA (an equivalent of 2×10^7 pfu of MVA) or PBS into the tumors on a weekly basis (Fig. 3A). Intratumoral injections of Heat-iMVA resulted in tumor eradication and 100% survival of the mice (Fig. 3, B and C). By contrast, all of the mice that received intratumoral injections of PBS had continued tumor growth, and were euthanized at 19 or 21 days post tumor implantation (Fig. 3, B and C).

To test whether mice whose tumors regressed after Heat-iMVA treatment had developed systemic and long-lasting antitumor immunity, we re-implanted them by injecting a lethal dose of B16-F10 melanoma cells (1×10^5) intradermally to the contralateral side 8 weeks after the initial tumors were eradicated. Naïve mice that were never exposed to B16-F10 melanoma cells or Heat-iMVA were used as controls. The mice were followed for 70 days after the tumor implantation. 90% of Heat-iMVA-treated mice survived the tumor challenge, whereas all of the naïve mice developed growing tumors and were eventually euthanized (Fig. 3D).

To test whether Heat-iMVA-treated mice developed systemic anti-tumor immunity in a different organ system, Heat-iMVA-treated mice were given an intravenous delivery of 1×10^5 B16-F10 melanoma cells. Mice were euthanized at 3 weeks post tumor challenge. The lungs of the mice were collected and fixed in formalin. The tumors on the surface of the lungs were visualized under a dissecting microscope and counted. Whereas all of the naïve mice developed lung surface tumors (with an average of 58 tumors per mouse), only one out of ten Heat-iMVA-treated mice developed 2 small tumor foci visible under the microscope, and the rest of the Heat-iMVA-treated mice were tumor free (Figure 3E). Collectively, these results indicate that intratumoral injection of Heat-iMVA leads to both eradication of injected tumors and to the development of therapeutic systemic antitumoral immunity.

Intratumoral injection of Heat-iMVA or UV-iMVA is highly potent therapeutically and elicits systemic antitumor immunity in a MC38 colon adenocarcinoma model

To test whether Heat-iMVA and UV-iMVA were active in a different solid tumor model, we intradermally implanted 5×10^5 MC38 colon cancer cells into the right flank of C57B/6 mice. Tumors were allowed to grow for 5 days, after which Heat-iMVA or UV-iMVA (equivalents of 2×10^7 pfu of MVA) or PBS control were injected into the tumor on a bi-weekly schedule (Fig. 3F). Whereas all of the PBS control mice died due to tumor growth (Fig. 3, G and J), 70% of Heat-iMVA-treated mice and 71% of UV-iMVA-treated mice survived at the end of the experiment (~60 days after virus injection) (Fig. 3, H-J).

To gauge whether the survivors had developed antitumor immunity, we challenged the mice with a lethal intradermal dose of MC38 cells (1×10^5) on the contralateral side. Whereas all of the naïve mice developed tumors and died, 100% of the Heat-iMVA and UV-iMVA-treated mice rejected the tumor challenge (Fig. 3K). Thus, Heat-iMVA and UV-iMVA are effective against two solid tumor models: melanoma and colon adenocarcinoma.

Intratumoral injection of Heat-iMVA leads to immunological changes in the tumor microenvironment and tumor-draining lymph nodes (TDLNs)

To investigate the immunologic changes within the B10-F10 melanoma tumors induced by intratumoral injection of Heat-iMVA, we harvested tumors at 3 days post-injection of Heat-iMVA or PBS and then assessed the immune cell infiltrates by FACS. The percentages of $CD3^+$ $CD45^+$ T cells among the live cells, $CD8^+$ or $CD4^+$ T cells expressing Granzyme B or Ki-67 increased in Heat-iMVA-treated tumors compared with those in PBS-treated tumors. By contrast, we found that the $CD4^+$ $Foxp3^+$ T cells out of $CD4^+$ T cells decreased in Heat-iMVA-treated tumors compared with those in PBS-treated tumors (Fig. 4, A-L). The absolute numbers of $CD3^+$, $CD8^+$, $CD4^+$ $Foxp3^-$ cells were dramatically increased in the Heat-iMVA-injected tumors compared with PBS control (Figure 4, M). In addition, the absolute numbers of $CD8^+$ Granzyme B^+ and $CD8^+$ Ki-67^+, as well as $CD4^+$ Granzyme B^+ and $CD4^+$ Ki-67^+ were also significantly increased in the Heat-iMVA-injected tumors compared with PBS control (Figure 4, N). These results indicate that intratumoral injection of Heat-iMVA triggered immunological changes in the tumor microenvironment, manifested as proliferation and activation of cytotoxic $CD4^+$ and $CD8^+$ T cells and reduction of percentages of $CD4^+$ $FoxP3^+$ regulatory T cells out of $CD4^+$ T cells. Heat-iMVA also led to increase in the percentages of $CD4^+$ and $CD8^+$ cells expressing proliferation (Ki-67) and lytic marker (granzyme B) in the tumor-draining lymph nodes (Fig. S5, A-H).

$CD8^+$ T cells are necessary for antitumor activity of Heat-iMVA

We performed antibody depletion experiments to determine which immune cell types are required for the therapeutic effect of Heat-iMVA in the melanoma model (Fig. 5A). Mice were treated with intraperitoneal administration of anti-CD4, anti-CD8a, anti-NK/NKT cell, or isotype control antibodies one day prior to intratumoral injection of viruses and twice a week thereafter until the mice died or tumors were eradicated. Whereas intratumoral delivery of Heat-iMVA in control mice led to regression of tumors, depletion of $CD8^+$ T cells abrogated the efficacy of Heat-iMVA and resulted in 100% lethality at three weeks (Fig. 5, B-F). Depletion of $CD4^+$ and NK/NKT cells resulted in only partial loss of efficacy

of Heat-iMVA (Fig. 5, B, F, G). To test whether CD4 and NK/NKT cell depletion during the intratumoral injection of viruses affected the abilities of the mice to generate systemic immunity, we rechallenged the surviving mice 4 months later with B16-F10 melanoma (1×10^5 cells) implanted intradermally at the contralateral flank. Although $CD4^+$ T cells were not strictly required for Heat-iMVA control of the initial melanoma, they were critical for the development of long-lasting adaptive immunity against tumor rechallenge by the surviving anti-CD4-treated mice (Fig. 5, H and I). By contrast, mice successfully treated with Heat-iMVA in the presence or absence of NK/NKT-depleting antibody efficiently rejected a tumor rechallenge (Fig. 5, H-I).

Heat-iMVA is more effective than MVA in eradicating non-injected tumors in a bilateral murine B16 melanoma model

We next compared intratumoral injection of Heat-iMVA vs. MVA in a bilateral B16-F10 melanoma implantation model. B16-F10 melanoma cells were implanted intradermally to the left and right flanks of C57B/6 mice (5×10^5 to the right flank and 1×10^5 to the left flank). 6 days after tumor implantation, we initiated biweekly injections of 2×10^7 pfu of MVA or an equivalent amount of Heat-iMVA into the larger tumors on the right flank (Fig. 6A). In mice treated with PBS, tumors grew rapidly on the right flank, which resulted in early death (Fig. 6, B-D). Intratumoral injection of either Heat-iMVA or MVA resulted in delayed tumor growth and improved survival compared with PBS (Fig. 6B). Intratumoral injection of Heat-iMVA was more effective than MVA in eradicating injected tumors and delaying or inhibiting the growth of non-injected tumors at the contralateral side (Fig. 6, E-H). We also observed improved survival in Heat-iMVA-treated mice compared with MVA-treated mice (Fig. 6B).

To understand the immune mechanisms underlying the superiority of Heat-iMVA over MVA in the induction of systemic antitumor immunity, we investigated the immune cell infiltrates in the non-injected tumors in Heat-iMVA or MVA-treated mice. We intradermally implanted 2.5×10^5 B16-F10 melanoma cells to the left flank and 5×10^5 B16-F10 melanoma cells to the right flank of the mice. Seven days post implantation, we injected either 2×10^7 pfu of MVA, or an equivalent amount of Heat-iMVA, or PBS into the larger tumors on the right flank. The injection was repeated three days later. The non-injected tumors were harvested and cell suspensions were generated. The live immune cell infiltrates in the tumors were analyzed by FACS. We observed 5- to 10-fold increases of $CD45^+$, $CD3^+$, $CD8^+$, and $CD4^+$ cells in the non-injected tumors of mice treated with Heat-iMVA compared with those in mice treated with PBS (Fig. 6I). MVA was less potent than Heat-iMVA in the induction of immune cells in the non-injected tumors (Fig. 6I). Heat-iMVA-treatment is more potent than MVA in the recruitment and induction of proliferation of cytotoxic Granzyme B-expressing $CD8^+$ and $CD4^+$ T cells in the non-injected tumors (Fig. 6J). These results indicate that intratumoral delivery of Heat-iMVA is more effective than MVA in the recruitment and activation of a variety of immune cells, especially with Granzyme B^+ $CD8^+$ T cells in the non-injected tumors. This correlates with its enhanced efficacy in eradicating or delaying the growth of non-injected tumors and prolongation of survival compared with MVA.

Intratumoral injection of Heat-iMVA is less effective in eradicating B16 melanomas in STING-deficient mice or Batf3-deficient mice than in wild-type controls

The STING pathway plays an important role in spontaneous T cell responses against tumors as well as in radiation-induced antitumoral immunity (7, 8, 25). BATF3 is a transcription factor that is critical for the development of $CD103^+/CD8\alpha^+$ lineage DCs, which play an important role in cross-presentation of viral and tumor antigens (26, 27). Batf3-deficient mice are unable to reject highly immunogenic tumors (26). To test whether STING or Batf3 plays a role in Heat-iMVA-mediated tumor clearance, we implanted B16-F10 melanoma cells intradermally into the right flank of WT C57B/6, $STING^{Gt/Gt}$, or $Batf3^{-/-}$ mice. At 11 days post-implantation, the tumors were injected with either Heat-iMVA (equivalent of 2×10^7 pfu) or PBS twice weekly. The initial tumor volumes at the time of first injections were shown. $Batf3^{-/-}$ mice had larger tumors than the other groups (fig. S6A). We found that 100% of the WT mice treated with Heat-iMVA were alive at 6 weeks, only 7.7% of STING-deficient mice treated with Heat-iMVA survived (Fig. 7A). All of the WT PBS control mice died (median survival of 24 days), as did all of the PBS-treated STING-deficient mice treated (median survival of 21 days) (Fig. 7A). Heat-iMVA treatment in $STING^{Gt/Gt}$ mice extended median survival to 28 days (Fig. 7A). All of the $Batf3^{-/-}$ mice died regardless of whether they were treated with Heat-iMVA or PBS. However, Heat-iMVA treatment in $Batf3^{-/-}$ mice extended the median survival from 21 to 30 days (Fig. 7A).

We proceeded to test the roles of STING and Batf3 in the efficacy of intratumoral Heat-iMVA in the bilateral B16-F10 melanoma model. The initial tumor volumes of the injected and non-injected sides were shown (fig. S6B). In the PBS-treated group, all of the mice died with a median survival of 16 days (Fig. 7B). Heat-iMVA eradicated all of the injected tumors, but the non-injected tumors were cured in only in 3 out of 10 WT mice (Fig. 7B). The median survival in Heat-iMVA-treated WT mice was 30 days, which was significantly extended compared with PBS-treated mice. Heat-iMVA failed to elicit significant therapeutic benefits in $Batf3^{-/-}$ mice (Fig. 7B). In STING-deficient mice, intratumoral injection of Heat-iMVA led to the delay of tumor growth and extension of median survival with a median survival of 21.5 days, but it was less effective compared with Heat-iMVA treatment in WT mice (Fig. 7B). We conclude that Batf3 is required for the induction of antitumor immunity by intratumoral delivery of Heat-iMVA. Based on the current knowledge on Batf3, we surmise that Batf3-dependent DCs are important for cross-presenting tumor antigens in this model. The STING DNA-sensing pathway also plays an important role in Heat-iMVA-induced adaptive antitumor immunity.

Batf3-dependent DCs are crucial in the generation of anti-tumor $CD8^+$ and $CD4^+$ T cells in both injected and non-injected tumors in response to Heat-iMVA treatment

Given the importance of Batf3-dependent DCs in Heat-iMVA-induced antitumor immunity, and the critical role of $CD8^+$ and $CD4^+$ T cells in Heat-iMVA-mediated antitumor effects, we investigated whether there is a deficiency in the generation of antitumor $CD8^+$ and $CD4^+$ T cells in Batf3 KO mice in response to intratumoral injection of Heat-iMVA using a bilateral tumor implantation model. We found that the absolute numbers of $CD3^+$, $CD8^+$ T cells, $CD4^+$ $Foxp3^-$ T cells per grams of injected or non-injected tumors increased in Heat-iMVA-treated WT mice compared with PBS-treated WT mice (Fig. 7, C and D). Similar

increase was seen with the ratios of CD8+/Treg and Tcon/Treg (Figure 7, C and D). By contrast, in Batf3 KO mice, Heat-iMVA-treatment did not result in significant increase in the absolute numbers of $CD3^+$, $CD8^+$ T cells, $CD4^+$ $Foxp3^-$ T cells per grams of injected or non-injected tumors (Fig. 7. C, D). The ratios of $CD8^+$/Treg and Tconv/Treg in the injected and non-injected tumors only marginally increased after Heat-iMVA treatment in $Batf3^{-/-}$ mice (Fig. 7, C and D). These results highlight an indispensible role for Batf3-dependent DCs for the antitumor efficacy induced by Heat-iMVA.

To test whether intratumoral injection of Heat-iMVA leads to the induction of activated tumor-specific $CD8^+$ T cells and whether Batf3-dependent $CD103^+/CD8\alpha^+$ DCs are involved in cross-priming of tumor antigens, we used a tyrosinase related protein-2 (TRP-2) tetramer assay to detect $CD8^+$ T cells that react to the melanocytic antigen TRP-2 immunogenic peptide. Briefly, WT C57B/6 and $Batf3^{-/-}$ mice were intradermally implanted with B16-F10. When the tumors were 4 mm in diameter, they were treated with intradermal injections of Heat-MVA twice with three days apart. 7 days post the initial injection, TDLNs were collected and cell suspensions were prepared and incubated with anti-FcγR II antibody and TRP2 tetramer, followed by staining with anti-CD3 and anti-CD8 antibodies. Intratumoral injection of Heat-MVA led to the increase in the percentages of TRP-2 tetramer positive $CD8^+$ T cells in the TDLNs compared with PBS control (fig. S8, A and B). This induction was diminished in Batf3-deficient mice (fig. S8, A and B). These results indicate that intratumoral injection with Heat-iMVA results in anti-tumor-specific $CD8^+$ T cell responses, which requires Batf3-dependent $CD103^+/CD8\alpha^+$ DCs.

STING also plays a role in the generation of antitumor $CD8^+$ T cell responses

We analyzed tumor infiltrating lymphocytes in both injected and non-injected tumors in PBS- or Heat-iMVA-treated STING-deficient mice and WT controls. Heat-iMVA induced smaller numbers of $CD3^+$, $CD8^+$ T cells, $CD4^+$ $Foxp3^-$ T cells per grams of injected or non-injected tumors in $STING^{Gt/Gt}$ mice compared with those in WT mice (Fig. 7. E and F). The ratios of $CD8^+$/Treg and Tconv/Treg in the Heat-iMVA-injected tumors in $STING^{Gt/Gt}$ mice were increased to a lesser extent than in WT mice (Fig. 7, C-D). These results indicate that STING also contributes to the generation of antitumor immunity in response to intratumoral injection of Heat-iMVA.

Combination of intratumoral Heat-iMVA and systemic immune checkpoint blockade results in synergistic anti-tumor therapeutic effects

We queried whether intratumoral injection of Heat-iMVA would have synergistic effects with immune checkpoint blockade in the bilateral melanoma model described above. 8 days after tumor implantation, we began injecting Heat-iMVA or PBS into the larger tumors on the right flank twice weekly. Four groups of mice were treated with Heat-iMVA, with each group receiving intraperitoneal delivery of either the isotype control, or anti-CTLA-4, or anti-PD-1, or anti-PD-L1 antibodies (Fig. 8A). Whereas the PBS-treated mice died quickly with increasing tumor growth over the next 20 days (Fig. 8. B, C, and D), the mice treated with Heat-iMVA+isotype control eliminated the injected tumors and delayed the growth of non-injected tumors at the contralateral side (Fig. 7E and F). As a result, treatment with Heat-iMVA+isotype significantly extended their survival compared with the PBS group

(Fig. 8B). The combination of intratumoral injection of Heat-iMVA and systemic delivery of anti-CTLA-4, anti-PD-1 and anti-PD-L1 antibodies further delayed or eliminated the non-injected tumors. As a result, 50% of mice treated with Heat-iMVA+anti-CTLA-4, 50% of mice treated Heat-iMVA+anti-PD-1, and 70% of mice treated with Heat-iMVA+anti-PD-L1 were tumor free at 58 days post-treatment, whereas 10% of mice treated with Heat-iMVA +isotype were tumor free (Fig. 8E-L). The ability to control the growth of non-injected distant tumors correlated with the improved survival in the combination group with Heat-iMVA+immune checkpoint blockade compared with Heat-iMVA+isotype control (Fig. 8B). Intraperitoneal delivery of anti-CTLA-4, anti-PD-1, or anti-PD-L1 alone had minimal therapeutic benefits in the B16-F10 melanoma model (fig. S8). Similar synergistic effects between intratumoral delivery of Heat-iMVA and systemic delivery of immune checkpoint blockade were also observed in MC38 colon adenocarcinoma bilateral tumor implantation model (Fig. S9). These results indicate that intratumoral delivery of Heat-iMVA overcomes treatment resistance to immune checkpoint blockade in a metastatic B16 melanoma model, leading to improved anti-tumor effects.

Intratumoral Heat-iMVA is superior to TLR agonist poly (I:C) in treating large established tumors alone and in combination with immune checkpoint blockade

Poly (I:C), a synthetic dsRNA, is an innate immune agonist. Extracellular poly (I:C) can activate the endosomal localized Toll-like receptor 3 (TLR3), whereas intracellular poly (I:C) can activate the cytosolic dsRNA sensor Melanoma Differentiation-Associated protein 5 (MDA5). Because $CD103^+$ DC in the tumor microenvironment and $CD8\alpha^+$ DC in the tumor draining lymph nodes express higher levels of TLR3, poly (I:C) could be an effective immune modulator for the cross-presenting DCs (28). We compared the anti-tumor efficacy of intratumoral injection of Heat-iMVA with poly (I:C) in a large established B16-OVA unilateral tumor implantation model. B16-OVA melanoma cells that constitutively express ovalbumin (OVA) (5×10^5 cells) were implanted intradermally into the shaved skin on the right flank of WT C57BL/6J mice. After 9 days post implantation, tumor sizes were measured and tumors that are 5–6 mm in diameter were injected with Heat-iMVA or poly (I:C), or with PBS twice weekly (fig. S10A). Intratumoral injection of Heat-iMVA or poly (I:C) was efficacious in delaying tumor growth in all of the treated mice (fig. S10B). The initial tumor volumes at the time injections were started were similar in each experimental group, with an average tumor volume of 45 mm^3 (fig. S10C). The median survival of Heat-iMVA-treated mice was extended from 9 days to 26.5 days (fig. S10D). Intratumoral injection of poly I:C (50 μg per mouse) twice weekly also led to tumor shrinkage (fig. S11B). It also extended the median survival from 9 days in PBS-treated mice to 17 days in poly (I:C)-treated mice (fig. S10D). Poly (I:C) appeared to be less potent than Heat-MVA (fig. S10D). In addition, mice treated with poly (I:C) exhibited systemic illness including fatigue and wasting. It is possibly that intratumorally delivered poly (I:C) was leaked into the systemic circulation which caused immune-related side effects. The results from this experiment showed that intratumoral injection of Heat-iMVA is effective in treating large established highly aggressive B16-OVA in a unilateral implantation model.

We further tested whether the combination of intratumoral injection of Heat-iMVA and systemic delivery of immune checkpoint blockade such as anti-CTLA-4, anti-PD-1, or anti-

PD-L1 antibodies have enhanced potency in eradicating large established B16-F10 in an unilateral tumor implantation model. Briefly, B16-F10 melanoma cells (5×10^5 cells) were implanted intradermally into the shaved skin on the right flank of WT C57BL/6J mice. After 9 days post implantation, tumors that are 5–6 mm in diameter were injected with Heat-iMVA or PBS. The mice were also treated with intraperitoneal delivery of anti-CTLA-4 antibody (100 μg per mouse), anti-PD-1 antibody (250 μg per mouse), anti-PD-L1 (200 μg per mouse), or isotype antibody twice weekly. Intratumoral injection of Heat-MVA was efficacious in delaying tumor growth in all of the treated mice and in eradicating the tumor in one tenth of the treated mice. It also extended the median survival from 6 days in PBS-treated mice to 27 days in Heat-treated mice (fig. S11 A, B and G). The mean initial tumor volumes at the time injections were started 76 mm^3 in the PBS group and 55 mm^3 in the Heat-MVA + isotype group (fig. S11F). Intratumoral injection of Heat-MVA in the presence of immune checkpoint blockade anti-CTLA-4 or anti-PD-1 cured 4 out of 10 treated mice, (fig. S11, C, D, and G), whereas the combination of intratumoral injection of Heat-MVA and anti-PD-L1 resulted in 80% of cure of large established tumors (fig. S11, E and G). These results showed that the combination of intratumoral injection of Heat-MVA with immune checkpoint blockade is more effective than virotherapy alone in treating large established poorly immunogenic B16-F10 in a unilateral implantation model. The combination of Heat-iMVA with anti-PD-L1 antibody seems to be the most potent of all of the combinations tested in this model.

Discussion

Poxviruses, such as engineered vaccinia viruses, have been investigated as oncolytic therapy for metastatic cancers (29). In this study, we took a different approach from traditional oncolytic viral therapy by using inactivated MVA (iMVA) to achieve anti-cancer therapeutic effects through the induction of innate immune responses in both infected tumors and immune cells within the tumors. Our results demonstrate that intratumoral injection of iMVA leads to efficient tumor eradication as well as the generation of systemic long-lasting antitumor immunity. Using STING or Batf3-deficient mice, we showed that the iMVA-mediated therapeutic effect depends on the cytosolic DNA-sensing pathway and Batf3-dependent $CD103^+/CD8\alpha^+$ DCs.

We attribute iMVA's antitumor activity to three key properties as follows: (i) iMVA is a potent inducer of type I IFN as well as proinflammatory cytokines and chemokines in cDCs and melanoma cells; (ii) iMVA infection of cDCs induces DC maturation and the expression of MHC class I on melanoma cells; and (iii) intratumoral injection of iMVA leads to alteration of the tumor suppressive microenvironment with the recruitment, activation, and proliferation of $CD8^+$ and $CD4^+$ T cells, as well as the reduction of the percentage of Tregs among $CD4^+$ T cells within the tumors.

Using BMDCs from various genetic KO mice, we demonstrated that iMVA-induced type I IFN gene expression and protein secretion from cDCs are dependent on the cGAS/STING/IRF3/IRF7 pathway. We showed previously that: (i) Heat-inactivated vaccinia virus infection of human or murine plasmacytoid dendritc cells (pDCs) induces type I IFN whereas live vaccinia virus does not; and (ii) Heat-inactivated vaccinia enters pDCs via the viral entry-

fusion complex (19). We infer that heat-iMVA is similarly taken up by cDCs via macropinocytosis, after which it accesses the cytosol through the viral entry-fusion complex. Some of the viral DNAs in the cytosol are sensed by cGAS (30–33), which leads to activation of STING and downstream transcriptions factors IRF3 and IRF7, resulting in the activation of IFN gene expression. Heat-iMVA induces higher levels of type I IFN in cDCs than MVA, which is likely due to the lack of expression of viral inhibitors of innate immune signaling.

It was reported recently that tumor DNA could be detected by the cytosolic DNA-sensing pathway mediated by STING/IRF3, which leads to spontaneous $CD8^+$ T cell priming (7). Mice deficient in STING or IRF3 were incapable of rejecting immunogenic tumors. Furthermore, STING-deficient mice were resistant to the combination immunotherapy with anti-CTLA-4 and anti-PD-L1, partly because tumor-specific T cells failed to expand in STING-deficient host (7). Intratumoral delivery of murine STING agonist DMXAA also showed efficacy in tumor eradication in a B16.SIY model, which is dependent on STING (25). However, human STING is insensitive to DMAXX stimulation, which explains of the failure of DMXAA in clinical trials (34). By contrast, synthetic cyclic dinucleotides (CDN) can act as human STING agonists, and preclinical studies showed that intratumoral delivery of CDN elicits antitumor effects in a B16 melanoma model in a STING-dependent manner (25). Our studies demonstrate that STING is also important in iMVA-induced anti-tumor therapeutic effects. STING-deficient mice were much less adept than WT mice at eradicating tumors in response to Heat-iMVA. Yet, the median survival was longer in the Heat-iMVA-treated STING-deficient mice compared with PBS-mock treated group, which suggests that Heat-iMVA might trigger other innate immune sensing mechanisms to extend survival in STING-deficient mice. Immune profiling of injected and non-injected tumors revealed that Heat-iMVA-treatment leads to the increase of $CD8^+$ and $CD4^+$ T cells, which is reduced in STING-deficient mice.

Our results demonstrate Batf3 plays an important role in determining the effectiveness of Heat-iMVA. Batf3 is a transcription factor highly expressed in cDCs and $Batf3^{-/-}$ mice have a selective defect in $CD103^+$ DCs in the peripheral tissues and $CD8\alpha^+$ DCs in the lymphoid organs (26, 27). Batf3-dependent $CD103^+/CD8\alpha^+$ DCs are required for spontaneous cross-priming of tumor antigen-specific $CD8^+$ T cells (26, 35–37). Broz et al. reported that $CD103^+$ DCs are sparsely present within the tumors and they compete for tumor antigens with abundant tumor-associated macrophages. $CD103^+$ DCs are uniquely capable in stimulating naïve as well as activated $CD8^+$ T cells and are critical for the success of adoptive T cell therapy (38). Spranger et al. reported that the activation of oncogenic signaling pathway WNT/β-catenin leads to reduction of $CD103^+$ DCs and anti-tumor T cells within the tumors. Intratumoral delivery of Flt3L-cultured BMDCs leads to responsiveness to the combination of anti-CTLA-4 and anti-PD-L1 immunotherapy (37). Systemic administration of Flt3L, a growth factor for $CD103^+$ DCs, and intratumor injection of poly I:C (TLR3 agonist) expanded and activated the $CD103^+$ DC populations within the tumors and overcome resistance or enhance responsiveness to immunotherapy in a murine melanoma and MC38 colon cancer models (28, 39). Interestingly, in the absence of poly I:C, in Flt3L-treated mice, CD103+ DCs remain immature although their numbers have increased due to Flt3L effects on the expansion of DC progenitor cells as well as $CD103^+$

DC differentiation (28). We envision that intratumoral delivery of iMVA leads to the maturation of $CD103^+$ DCs and promotes their ability to cross-present tumor antigens to naïve or activated $CD8^+$ T cells. In mice that are devoid of $CD103^+$ DCs, intratumoral delivery of iMVA fails to induce activated $CD8^+$ T cells in both injected and non-injected tumors (Figure 7, C and D). We also observed a reduction of recruitment and proliferation of $CD4^+$ T cells and Tconv/Treg ratio in response to Heat-iMVA therapy in both injected and non-injected tumors in $Batf3^{-/-}$ mice compared with WT mice. We hypothesize that the initial tumor cell killing mediated by activated $CD8^+$ T cells might be important for providing tumor antigens for presentation by other types of antigen-presentation cells for the generation of antitumor $CD4^+$ T cell responses.

The limitations of this study include the use of two transplantable murine tumor models, B16-F10 and MC38, both of which have numerous somatic mutations and neoantigens (40, 41). It is plausible that the observed efficacy with Heat-iMVA in these tumor models is related to the abundance of neoantigens. It is also plausible that the pre-existing immune cells within the tumors including DCs and tumor-associated-macrophages (TAMs) might play a role in influencing the response to treatment. These studies should be extended to investigate the efficacy of Heat-iMVA in more tumor histological types, including breast and prostate cancers, which are more resistant to immunotherapy than melanoma. Our results on Batf3 KO mice indicate that Batf3-dependent DCs are important for Heat-iMVA-induced antitumor effects, but it does not exclude the possibility that other myeloid cells might be involved. Future studies will monitor the dynamic changes of myeloid cells, including $CD103^+$ DCs, $CD11b^+$ DCs, monocytes, neutrophils, and TAMs, in the injected and non-injected tumors and TDLNs in response to iMVA. We observed that the majority of the surviving mice after iMVA-treatment developed long-lasting adaptive immunity against tumor rechallenge at contralateral flank or through intravenous delivery. The mechanistic details warrant further investigation.

Traditional oncolytic viral therapy relies on tumor-selective viral replication to kill tumor cells in addition to other mechanisms of action, including the induction of antitumor immunity and disruption of tumor-associated vasculature through viral replication in endothelial cells (1, 29, 42). Our results demonstrate that intratumoral delivery of non-replicative immune stimulating iMVA can provide alternative mechanisms of tumor killing through the generation of antitumor $CD8^+$ and $CD4^+$ effector and likely memory cells. Although depletion of $CD8^+$ T cells leads to ineffective virotherapy, depletion of $CD4^+$ T cells renders the surviving mice unable to defend against tumor re-challenge. In addition, the combination of virotherapy with immune checkpoint blockade, which relieves the T cell inhibitory mechanisms, leads to more efficient tumor killing and improved survival than either virotherapy alone or immune checkpoint blockade alone.

Since the initial approval of ipilimumab, an anti-CTLA-4 antibody, by the US FDA for the treatment of metastatic melanoma in 2011, additional immune checkpoint blocking antibodies (anti-PD-1 and anti-PD-L1) have been approved for the treatment of melanoma, as well as other cancers, including non-small cell lung cancer, bladder and renal cancer (14–16). Despite these successes in some patients using checkpoint blockade immunotherapy, the majority of patients fail to respond to immunotherapy alone, and therefore further

investigations of mechanisms underlying resistance to immunotherapy and the development of novel combinatorial approaches are needed. Our study demonstrated that intratumoral injection of iMVA and systemic delivery of immune checkpoint blockade antibodies elicits synergistic antitumor effects. We envision that this approach can be used in several clinical settings: (i) for patients who have metastatic cancers that are otherwise unresponsive to immunotherapy; (ii) for patients who have a partial response to immunotherapy and still have active symptomatic tumor burden; and (iii) for patients who initially responded to immunotherapy but have acquired resistance. Finally, we believe that genetic engineering of MVA virus to remove immune suppressive genes, such as E3L, and to express immune modulatory gene(s) will further improve its therapeutic efficacy.

Materials and Methods

Study design

Our research objective was to determine the efficacy of intratumoral delivery of inactivated MVA (iMVA) as monotherapy or in combination with systemic delivery of immune checkpoint blockade for solid tumors. We used unilateral and bilateral tumor implantation models to assess the responsiveness to iMVA in the presence or absence of immune checkpoint blockade. We also determined the contribution of cytosolic DNA-sensing pathway and $CD103^{+}$/ $CD8\alpha^{+}$ DCs in iMVA-induced antitumor effects using $STING^{Gt/Gt}$ and $Batf3^{-/-}$ mice. In all experiments, animals were assigned to various experimental groups in random. For survival studies, sample sizes of 8–10 mice were used and the experiments were repeated two to three times. For experiments designed to evaluate the tumor immune cell infiltrates, 3–5 mice were used for each experiment and the experiments were repeated two to three times. For in vitro experiments designed to assess the induction of type I IFN and proinflammatory cytokines and chemokines, triplicate samples were used and the experiments were repeated at least twice.

Viruses and Cell lines

MVA virus was kindly provided by Gerd Sutter (University of Munich), propagated in BHK-21 (baby hamster kidney cell, ATCC CCL-10) cells. Viruses were purified through a 36% sucrose cushion. Heat-MVA was generated by incubating purified MVA virus at 55°C for 1 hour. For generation of UV-MVA, MVA was UV irradiated in a Stratalinker 1800 UV cross-linker (Stratagene) with a 365 nm UV lamp for 15 min. BHK-21 were cultured in Eagle’s Minimal Essential Medium (Life Technologies, Cat# 11095-080) containing 10% FBS, 0.1 mM nonessential amino acids (NEAA), and 50 mg/ml gentamycin. The murine melanoma cell line B16-F10 was originally obtained from I. Fidler (MD Anderson Cancer Center). The MC38 colon adenocarcinoma cancer cells were originally obtained from ATCC. Both B16-F10 and MC38 cells were maintained in RPMI 1640 medium supplemented with 10% FBS, penicillin and streptomycin.

Mice

Female C57BL/6J mice between 6 and 10 weeks of age were purchased from the Jackson Laboratory (Stock # 000664) and were used for the preparation of bone marrow-derived dendritic cells and for in vivo experiments. These mice were maintained in the animal

facility at the Sloan Kettering Institute. All procedures were performed in strict accordance with the recommendations in the Guide for the Care and Use of Laboratory Animals of the National Institute of Health. The protocol was approved by the Committee on the Ethics of Animal Experiments of Sloan-Kettering Cancer Institute. cGAS$^{-/-}$, IRF3$^{-/-}$, IRF7$^{-/-}$, IRF5$^{-/-}$, Batf3$^{-/-}$, and STING$^{Gt/Gt}$ mice were generated in the laboratories of Drs. Zhijian Chen (University of Texas Southwestern Medical Center; cGAS$^{-/-}$), Tadatsugu Taniguchi (University of Tokyo; IRF3$^{-/-}$ and IRF7$^{-/-}$), Tak Mak (University of Toronto; IRF5$^{-/-}$); Kenneth Murphy (Washington University; Batf3$^{-/-}$), and Russell Vance (University of California, Berkeley; STING$^{Gt/Gt}$). IFNAR1$^{-/-}$ mice were provided by Dr. Eric Pamer (Sloan Kettering Institute); the mice were purchased from B&K Universal and were backcrossed with C57BL/6 mice for more than six generations. IRF5$^{-/-}$ mice were backcrossed to C57BL/6J mice for at least six generations in Dr. Paula M. Pitha's laboratory before they were transferred to Sloan Kettering Institute.

RNA isolation and quantitative real-time PCR

RNA was extracted from whole-cell lysates with an RNeasy Mini kit (Qiagen) and was reverse transcribed with a First Strand cDNA synthesis kit (Fermentas). Quantitative real-time PCR was performed in triplicate with SYBR Green PCR Mater Mix (Life Technologies) and Applied Biosystems 7500 Real-time PCR Instrument (Life Technologies) using gene-specific primers. Relative expression was normalized to the levels of glyceraldehyde-3-phosphate dehydrogenase (GAPDH). The primer sequences for quantitative real-time PCR are listed in table S1.

Cytokine assays

Cells were infected with various viruses at a MOI of 10 for 1 h or mock infected. The inoculum was removed and the cells were washed with PBS twice and incubated with fresh medium. Supernatants were collected at various times post infection. Cytokine levels were measured by using enzyme-linked immunosorbent essay (ELISA) kits for IFN-α/β (PBL Biomedical Laboratories), IL-6, CCL4, and CCL5 (R & D systems).

Western Blot Analysis

Bone marrow-derived dendritic cells (BMDCs) were generated according to the protocol (Dai et al., 2014). BMDCs (1×10^6) from WT and KO mice were infected with MVA at a MOI (multiplicity of infection) of 10 or an equivalent amount of Heat-MVA, or UV-MVA. Whole-cell lysates were prepared. Equal amounts of proteins were subjected to sodium dodecyl sulfate-polyacrylamide gel electrophoresis and the polypeptides were transferred to a nitrocellulose membrane. Phosphorylation of IRF3, IRF3, and STING levels were determined using respective antibodies (Cell Signaling). Vaccinia E3 protein level was determined by using anti-E3 monoclonal antibody (MAb 3015B2) kindly provided by Dr. Stuart N. Isaacs (University of Pennsylvania) (43). Anti-glyceraldehyde-3-phosphate dehydrogenase (GADPH) or anti-β-actin antibodies (Cell Signaling) were used as loading controls. B16-F10 melanoma cells were infected with MVA at a MOI of 10 or with an equivalent amount of Heat-MVA. Cell lysates were collected at various times post infection. Western blot analysis was performed using anti-phospho-IRF3, anti-IRF3, and anti-GAPDH antibodies as described above.

Flow cytometry analysis of DC maturation

For DC maturation analysis, BMDCs were generated from WT and STING$^{Gt/Gt}$ mice and infected with MVA at a MOI of 10 or with an equivalent amount of Heat-iMVA. Cells were collected at 14 h post infection and were then fixed with Fix Buffer I (BD Biosciences) for 15 min at 37°C. Cells were washed, permeabilized with PermBuffer (BD Biosciences) for 30 min on ice, and stained with antibodies against MHC Class I, CD40, CD86, and CD80 for 30 min. Cells were analyzed using the LSRII Flow cytometer (BD Biosciences). Data were analyzed with FlowJo software (Treestar).

Unilateral intradermal tumor implantation and intratumoral injection with viruses

All mouse procedures were performed in strict accordance with the recommendations in the Guide for the Care and Use of Laboratory Animals of the National Institute of Health. The protocol was approved by the Committee on the Ethics of Animal Experiments of Sloan-Kettering Cancer Institute. B16-F10 melanoma (1×10^5 cells in a volume of 50 μl) were implanted intradermally into the shaved skin on the right flank of WT C57BL/6J mice. In some experiments, tumors were implanted to the right flank of STING$^{Gt/Gt}$, or Batf3$^{-/-}$, or age-matched WT controls. After 8–10 days post implantation, tumor sizes were measured and tumors that are 3 mm in diameter or larger will be injected with Heat-MVA (equivalent of 2×10^7 pfu of MVA in a volume of 50 μl) or PBS when the mice were under anesthesia. Viruses were injected weekly or twice weekly as specified in each experiment. Mice were monitored daily and tumor sizes were measured twice a week. Tumor volumes were calculated according the following formula: l (length) × w (width)x h(height)/2. Mice were euthanized for signs of distress or when the diameter of the tumor reached 10 mm.

In some cases, 1×10^5 MC38 colon adenocarcinoma cells were implanted intradermally on the right flank of shaved mice. After 7 days, tumors were injected with either PBS, Heat-MVA, or UV-MVA at the same dose as described above twice weekly.

Tumor rechallenge to assess the development of systemic antitumor immunity

The survived mice (more than 60 days post initiation of intratumoral virotherapy) were rechallenged with either intradermally delivery of a lethal dose of B16-F10 (1×10^5 cells) at the contralateral side or by intravenous delivery of a lethal dose of B16-F10 (1×10^5 cells) and then euthanized at 3 weeks post rechallenge to evaluate the presence of tumors on the surface of lungs.

T cell depletion experiment

B16-F10 murine melanoma cells (1×10^5 cells in a volume of 50 μl) were implanted intradermally into the right flank of shaved WT C57B/6 mice at 6–8 weeks of age. At 8 days post tumor implantation, the tumors were injected with either Heat-MVA (an equivalent dose of 2×10^7 pfu of MVA) or PBS twice weekly. Depletion antibodies for CD4$^+$, CD8$^+$ and NK cells (200 μg of GK1.5, 2.43, and PK136) (Monoclonal Antibody Core Facility, MSKCC) (44) were injected intraperitoneally twice weekly starting one day prior to viral injection, and they were used until the animals either died, or were euthanized, or were completely clear of tumors. Mice were monitored daily and tumor sizes were measured. The depletion

of targeted immune cells was validated by FACS of peripheral blood of mice after 4 doses of antibodies.

Bilateral tumor implantation model and intratumoral injection with viruses in the presence or absence of systemic or intratumoral administration of immune checkpoint blockade

B16-F10 melanoma cells were implanted intradermally to the left and right flanks of C57B/6 mice (5×10^5 to the right flank and 1×10^5 to the left flank). 8 days after tumor implantation, we intratumorally inject 2×10^7 pfu of MVA or an equivalent amount of Heat-MVA to the larger tumors on the right flank. The tumor sizes were measured and the tumors were injected twice a week. The survival of mice was monitored.

In some experiments, MC38 colon adenocarcinoma cells were implanted intradermally to the left and right flanks of C57B/6 mice (5×10^5 to the right flank and 1×10^5 to the left flank).

In some experiments, $STING^{Gt/Gt}$, $Batf3^{-/-}$ mice and WT age-matched controls were used for bilateral B16-F10 melanoma implantation, and treated with PBS or Heat-MVA to the larger tumors on the right flank of the mice.

In some experiments, the mice with bilateral tumors were treated with intratumoral injection of Heat-MVA to the larger tumors on the right flank and intraperitoneal delivery of immune checkpoint blockade antibodies, including anti-CTLA-4, anti-PD-1, or anti-PD-L1.

Preparation of tumor cell suspensions

First we isolated injected and/or non-injected tumors using forceps and surgical scissors three days post second treatment and 7 days post first treatment with PBS, MVA or Heat-MVA. The tumors were then weighed. Tumors or tumor draining lymph nodes were minced prior to incubation with Liberase (1.67 Wünsch U/ml) and DNase (0.2mg/ml) for 30 minutes at 37°C. Cell suspensions were generated by repeated pipetting, filtered through a 70-μm nylon filter, and then washed with complete RPMI prior to Ficoll purification to remove dead cells.

Flow cytometry analysis of tumor infiltrating immune cells

In the unilateral tumor implantation model, 5×10^5 B16-F10 melanoma cells were implanted intradermally to the right flank of the mice. Seven days post implantation, either Heat-iMVA (an equivalent of 2×10^7 pfu of MVA) or PBS were injected into the tumors on the right flank. The injectionw were repeated three days later. Tumors and TDLNs were harvested 3 days post last injection and cell suspensions were generated.

In the bilateral tumor implantation model, B16-F10 melanoma cells were implanted intradermally to the left and right flanks for WT, $STING^{Gt/Gt}$, or $Batf3^{-/-}$ mice (5×10^5 cells to the right flank and 2.5×10^5 cells to the left flank). Either MVA or Heat-iMVA were injected to the larger tumors on day 7 and 10 after initial tumor implantation, and both the injected and non-injected tumors were harvested. Cell suspensions were generated according to the following protocol (45).

Cells were processed for surface labeling with anti-CD3, CD45, CD4, and CD8 antibodies. Live cells are distinguished from dead cells by using fixable dye eFluor506 (eBioscience). They were further permeabilized using FoxP3 fixation and permeabilization kit (eBioscience), and stained for Ki-67, FoxP3, and Granzyme B. Data were acquired using the LSRII Flow cytometer (BD Biosciences). Data were analyzed with FlowJo software (Treestar).

Statistics

Two-tailed unpaired Student's *t* test was used for comparisons of two groups in the studies. Survival data were analyzed by log-rank (Mantel-Cox) test. The p values deemed significant are indicated in the figures as follows: *, $p < 0.05$; **, $p < 0.01$; ***, $p < 0.001$; ****, $p < 0.0001$. The numbers of animals included in the study are discussed in each figure legend.

Reagents

The commercial sources for reagents were as follows: CpG oligodeoxynucleotide ODN2216 (Invitrogen); We used the following antibodies. Therapeutic anti-CTLA4 (clone 9H10 and 9D9), anti-PD1 (clone RMP1-14), anti-PD-L1 (clone 10F.9G2) were purchased from BioXcell; Antibodies used for flow cytometry were purchased from eBioscience (CD45.2 Alexa Fluor 700, CD3 PE-Cy7, CD4 APC-efluor780, CD8 PerCP-efluor710, FOXP3 Alexa Fluor 700, MHC Class I APC, CD40 APC, CD80 APC, CD86 APC), Invitrogen (CD4 QDot 605, Granzyme B PE-Texas Red, Granzyme B APC), BD Pharmingen (Ki-67-Alexa Fluor 488).

Supplementary Material

Refer to Web version on PubMed Central for supplementary material.

Acknowledgments

Funding: This work was supported that NIH grant K-08 AI073736 (L.D.), R56AI095692 (L.D.), Lucille Castori Center for Microbes, Inflammation & Cancer seed grant (L.D.), the Society of Memorial Sloan Kettering (MSK) research grant (L.D.), MSK Technology Development Fund (L.D.) LD is the recipient of a Physician Scientist Career Development Award from the Dermatology Foundation and a research scholar from American Skin Association. SS is an American Cancer Society Research Professor. C.S.T. was supported by the 2014 Carolyn L. Kuckein Student Research Fellowship. D.Z. is a Bart A. Kamen Fellow of the Damon Runyon Cancer Research Foundation. This work was supported in part supported by the Swim across America (J.D.W., T.M.), Ludwig Institute for Cancer Research (J.D.W., T.M.), National Cancer Institute grants R01 CA56821 (J.D.W). This research was also funded in part through the NIH/NCI Cancer Center Support Grant P30 CA008748. MVA virus was kindly provided by Gerd Sutter (University of Munich).

REFERENCES AND NOTES

1. Bell J, McFadden G. Viruses for tumor therapy. Cell host & microbe. 2014; 15:260–265. [PubMed: 24629333]
2. Lichty BD, Breitbach CJ, Stojdl DF, Bell JC. Going viral with cancer immunotherapy. Nature reviews. Cancer. 2014; 14:559–567. [PubMed: 24990523]
3. Kaufman HL, Kohlhapp FJ, Zloza A. Oncolytic viruses: a new class of immunotherapy drugs. Nat Rev Drug Discov. 2015; 14:642–662. [PubMed: 26323545]
4. Fuertes MB, Woo SR, Burnett B, Fu YX, Gajewski TF. Type I interferon response and innate immune sensing of cancer. Trends Immunol. 2013; 34:67–73. [PubMed: 23122052]

5. Fuertes MB, Kacha AK, Kline J, Woo SR, Kranz DM, Murphy KM, Gajewski TF. Host type I IFN signals are required for antitumor CD8+ T cell responses through CD8{alpha}+ dendritic cells. J Exp Med. 2011; 208:2005–2016. [PubMed: 21930765]
6. Diamond MS, Kinder M, Matsushita H, Mashayekhi M, Dunn GP, Archambault JM, Lee H, Arthur CD, White JM, Kalinke U, Murphy KM, Schreiber RD. Type I interferon is selectively required by dendritic cells for immune rejection of tumors. J Exp Med. 2011; 208:1989–2003. [PubMed: 21930769]
7. Woo SR, Fuertes MB, Corrales L, Spranger S, Furdyna MJ, Leung MY, Duggan R, Wang Y, Barber GN, Fitzgerald KA, Alegre ML, Gajewski TF. STING-dependent cytosolic DNA sensing mediates innate immune recognition of immunogenic tumors. Immunity. 2014; 41:830–842. [PubMed: 25517615]
8. Deng L, Liang H, Xu M, Yang X, Burnette B, Arina A, Li XD, Mauceri H, Beckett M, Darga T, Huang X, Gajewski TF, Chen ZJ, Fu YX, Weichselbaum RR. STING-Dependent Cytosolic DNA Sensing Promotes Radiation-Induced Type I Interferon-Dependent Antitumor Immunity in Immunogenic Tumors. Immunity. 2014; 41:843–852. [PubMed: 25517616]
9. Sutter G, Staib C. Vaccinia vectors as candidate vaccines: the development of modified vaccinia virus Ankara for antigen delivery. Current drug targets. Infectious disorders. 2003; 3:263–271. [PubMed: 14529359]
10. McCurdy LH, Larkin BD, Martin JE, Graham BS. Modified vaccinia Ankara: potential as an alternative smallpox vaccine. Clin Infect Dis. 2004; 38:1749–1753. [PubMed: 15227622]
11. Vollmar J, Arndtz N, Eckl KM, Thomsen T, Petzold B, Mateo L, Schlereth B, Handley A, King L, Hulsemann V, Tzatzaris M, Merkl K, Wulff N, Chaplin P. Safety and immunogenicity of IMVAMUNE, a promising candidate as a third generation smallpox vaccine. Vaccine. 2006; 24:2065–2070. [PubMed: 16337719]
12. Goepfert PA, Elizaga ML, Sato A, Qin L, Cardinali M, Hay CM, Hural J, DeRosa SC, DeFawe OD, Tomaras GD, Montefiori DC, Xu Y, Lai L, Kalams SA, Baden LR, Frey SE, Blattner WA, Wyatt LS, Moss B, Robinson HL. Phase 1 safety and immunogenicity testing of DNA and recombinant modified vaccinia Ankara vaccines expressing HIV-1 virus-like particles. J Infect Dis. 2011; 203:610–619. [PubMed: 21282192]
13. Gomez CE, Najera JL, Perdiguero B, Garcia-Arriaza J, Sorzano CO, Jimenez V, Gonzalez-Sanz R, Jimenez JL, Munoz-Fernandez MA, Lopez Bernaldo de Quiros JC, Guardo AC, Garcia F, Gatell JM, Plana M, Esteban M. The HIV/AIDS vaccine candidate MVA-B administered as a single immunogen in humans triggers robust, polyfunctional, and selective effector memory T cell responses to HIV-1 antigens. J Virol. 2011; 85:11468–11478. [PubMed: 21865377]
14. Topalian SL, Drake CG, Pardoll DM. Immune checkpoint blockade: a common denominator approach to cancer therapy. Cancer Cell. 2015; 27:450–461. [PubMed: 25858804]
15. Sharma P, Allison JP. The future of immune checkpoint therapy. Science. 2015; 348:56–61. [PubMed: 25838373]
16. Callahan MK, Postow MA, Wolchok JD. Targeting T Cell Co-receptors for Cancer Therapy. Immunity. 2016; 44:1069–1078. [PubMed: 27192570]
17. Zou W, Wolchok JD, Chen L. PD-L1 (B7-H1) and PD-1 pathway blockade for cancer therapy: Mechanisms, response biomarkers, and combinations. Science translational medicine. 2016; 8:328rv324.
18. Dai P, Wang W, Cao H, Avogadri F, Dai L, Drexler I, Joyce JA, Li XD, Chen Z, Merghoub T, Shuman S, Deng L. Modified vaccinia virus Ankara triggers type I IFN production in murine conventional dendritic cells via a cGAS/STING-mediated cytosolic DNA-sensing pathway. PLoS Pathog. 2014; 10:e1003989. [PubMed: 24743339]
19. Cao H, Dai P, Wang W, Li H, Yuan J, Wang F, Fang CM, Pitha PM, Liu J, Condit RC, McFadden G, Merghoub T, Houghton AN, Young JW, Shuman S, Deng L. Innate Immune Response of Human Plasmacytoid Dendritic Cells to Poxvirus Infection Is Subverted by Vaccinia E3 via Its Z-DNA/RNA Binding Domain. PLoS One. 2012; 7:e36823. [PubMed: 22606294]
20. Ishikawa H, Barber GN. STING is an endoplasmic reticulum adaptor that facilitates innate immune signalling. Nature. 2008; 455:674–678. [PubMed: 18724357]

21. Tanaka Y, Chen ZJ. STING specifies IRF3 phosphorylation by TBK1 in the cytosolic DNA signaling pathway. Sci Signal. 2012; 5:ra20. [PubMed: 22394562]
22. Gao P, Ascano M, Zillinger T, Wang W, Dai P, Serganov AA, Gaffney BL, Shuman S, Jones RA, Deng L, Hartmann G, Barchet W, Tuschl T, Patel DJ. Structure-function analysis of STING activation by c[G(2',5')pA(3',5')p] and targeting by antiviral DMXAA. Cell. 2013; 154:748–762. [PubMed: 23910378]
23. Xiao TS, Fitzgerald KA. The cGAS-STING pathway for DNA sensing. Mol Cell. 2013; 51:135–139. [PubMed: 23870141]
24. Sauer JD, Sotelo-Troha K, von Moltke J, Monroe KM, Rae CS, Brubaker SW, Hyodo M, Hayakawa Y, Woodward JJ, Portnoy DA, Vance RE. The N-ethyl-N-nitrosourea-induced Goldenticket mouse mutant reveals an essential function of Sting in the in vivo interferon response to Listeria monocytogenes and cyclic dinucleotides. Infection and immunity. 2011; 79:688–694. [PubMed: 21098106]
25. Corrales L, Glickman LH, McWhirter SM, Kanne DB, Sivick KE, Katibah GE, Woo SR, Lemmens E, Banda T, Leong JJ, Metchette K, Dubensky TW Jr, Gajewski TF. Direct Activation of STING in the Tumor Microenvironment Leads to Potent and Systemic Tumor Regression and Immunity. Cell reports. 2015; 11:1018–1030. [PubMed: 25959818]
26. Hildner K, Edelson BT, Purtha WE, Diamond M, Matsushita H, Kohyama M, Calderon B, Schraml BU, Unanue ER, Diamond MS, Schreiber RD, Murphy TL, Murphy KM. Batf3 deficiency reveals a critical role for CD8alpha+ dendritic cells in cytotoxic T cell immunity. Science. 2008; 322:1097–1100. [PubMed: 19008445]
27. Edelson BT, Kc W, Juang R, Kohyama M, Benoit LA, Klekotka PA, Moon C, Albring JC, Ise W, Michael DG, Bhattacharya D, Stappenbeck TS, Holtzman MJ, Sung SS, Murphy TL, Hildner K, Murphy KM. Peripheral CD103+ dendritic cells form a unified subset developmentally related to CD8alpha+ conventional dendritic cells. J Exp Med. 2010; 207:823–836. [PubMed: 20351058]
28. Salmon H, Idoyaga J, Rahman A, Leboeuf M, Remark R, Jordan S, Casanova-Acebes M, Khudoynazarova M, Agudo J, Tung N, Chakarov S, Rivera C, Hogstad B, Bosenberg M, Hashimoto D, Gnjatic S, Bhardwaj N, Palucka AK, Brown BD, Brody J, Ginhoux F, Merad M. Expansion and Activation of CD103(+) Dendritic Cell Progenitors at the Tumor Site Enhances Tumor Responses to Therapeutic PD-L1 and BRAF Inhibition. Immunity. 2016; 44:924–938. [PubMed: 27096321]
29. Kirn DH, Thorne SH. Targeted and armed oncolytic poxviruses: a novel multi-mechanistic therapeutic class for cancer. Nature reviews. Cancer. 2009; 9:64–71. [PubMed: 19104515]
30. Sun L, Wu J, Du F, Chen X, Chen ZJ. Cyclic GMP-AMP synthase is a cytosolic DNA sensor that activates the type I interferon pathway. Science. 2013; 339:786–791. [PubMed: 23258413]
31. Wu J, Sun L, Chen X, Du F, Shi H, Chen C, Chen ZJ. Cyclic GMP-AMP is an endogenous second messenger in innate immune signaling by cytosolic DNA. Science. 2013; 339:826–830. [PubMed: 23258412]
32. Li X, Shu C, Yi G, Chaton CT, Shelton CL, Diao J, Zuo X, Kao CC, Herr AB, Li P. Cyclic GMP-AMP synthase is activated by double-stranded DNA-induced oligomerization. Immunity. 2013; 39:1019–1031. [PubMed: 24332030]
33. Gao P, Ascano M, Wu Y, Barchet W, Gaffney BL, Zillinger T, Serganov AA, Liu Y, Jones RA, Hartmann G, Tuschl T, Patel DJ. Cyclic [G(2',5')pA(3',5')p] is the metazoan second messenger produced by DNA-activated cyclic GMP-AMP synthase. Cell. 2013; 153:1094–1107. [PubMed: 23647843]
34. Lara PN Jr, Douillard JY, Nakagawa K, von Pawel J, McKeage MJ, Albert I, Losonczy G, Reck M, Heo DS, Fan X, Fandi A, Scagliotti G. Randomized phase III placebo-controlled trial of carboplatin and paclitaxel with or without the vascular disrupting agent vadimezan (ASA404) in advanced non-small-cell lung cancer. J Clin Oncol. 2011; 29:2965–2971. [PubMed: 21709202]
35. Ginhoux F, Liu K, Helft J, Bogunovic M, Greter M, Hashimoto D, Price J, Yin N, Bromberg J, Lira SA, Stanley ER, Nussenzweig M, Merad M. The origin and development of nonlymphoid tissue CD103+ DCs. J Exp Med. 2009; 206:3115–3130. [PubMed: 20008528]
36. Zhang Y, Chen G, Liu Z, Tian S, Zhang J, Carey CD, Murphy KM, Storkus WJ, Falo LD Jr, You Z. Genetic Vaccines To Potentiate the Effective CD103+ Dendritic Cell-Mediated Cross-Priming of Antitumor Immunity. J Immunol. 2015; 194:5937–5947. [PubMed: 25972487]

37. Spranger S, Bao R, Gajewski TF. Melanoma-intrinsic beta-catenin signalling prevents anti-tumour immunity. Nature. 2015; 523:231–235. [PubMed: 25970248]

38. Broz ML, Binnewies M, Boldajipour B, Nelson AE, Pollack JL, Erle DJ, Barczak A, Rosenblum MD, Daud A, Barber DL, Amigorena S, Van't Veer LJ, Sperling AI, Wolf DM, Krummel MF. Dissecting the tumor myeloid compartment reveals rare activating antigen-presenting cells critical for T cell immunity. Cancer Cell. 2014; 26:638–652. [PubMed: 25446897]

39. Sanchez-Paulete AR, Cueto FJ, Martinez-Lopez M, Labiano S, Morales-Kastresana A, Rodriguez-Ruiz ME, Jure-Kunkel M, Azpilikueta A, Aznar MA, Quetglas JI, Sancho D, Melero I. Cancer Immunotherapy with Immunomodulatory Anti-CD137 and Anti-PD-1 Monoclonal Antibodies Requires BATF3-Dependent Dendritic Cells. Cancer Discov. 2016; 6:71–79. [PubMed: 26493961]

40. Yadav M, Jhunjhunwala S, Phung QT, Lupardus P, Tanguay J, Bumbaca S, Franci C, Cheung TK, Fritsche J, Weinschenk T, Modrusan Z, Mellman I, Lill JR, Delamarre L. Predicting immunogenic tumour mutations by combining mass spectrometry and exome sequencing. Nature. 2014; 515:572–576. [PubMed: 25428506]

41. Castle JC, Kreiter S, Diekmann J, Lower M, van de Roemer N, de Graaf J, Selmi A, Diken M, Boegel S, Paret C, Koslowski M, Kuhn AN, Britten CM, Huber C, Tureci O, Sahin U. Exploiting the mutanome for tumor vaccination. Cancer Res. 2012; 72:1081–1091. [PubMed: 22237626]

42. Breitbach CJ, Thorne SH, Bell JC, Kirn DH. Targeted and armed oncolytic poxviruses for cancer: the lead example of JX-594. Current pharmaceutical biotechnology. 2012; 13:1768–1772. [PubMed: 21740365]

43. Weaver JR, Shamim M, Alexander E, Davies DH, Felgner PL, Isaacs SN. The identification and characterization of a monoclonal antibody to the vaccinia virus E3 protein. Virus research. 2007; 130:269–274. [PubMed: 17583368]

44. Avogadri F, Merghoub T, Maughan MF, Hirschhorn-Cymerman D, Morris J, Ritter E, Olmsted R, Houghton AN, Wolchok JD. Alphavirus replicon particles expressing TRP-2 provide potent therapeutic effect on melanoma through activation of humoral and cellular immunity. PLoS One. 2010; 5

45. Zamarin D, Holmgaard RB, Subudhi SK, Park JS, Mansour M, Palese P, Merghoub T, Wolchok JD, Allison JP. Localized oncolytic virotherapy overcomes systemic tumor resistance to immune checkpoint blockade immunotherapy. Science translational medicine. 2014; 6:226ra232.

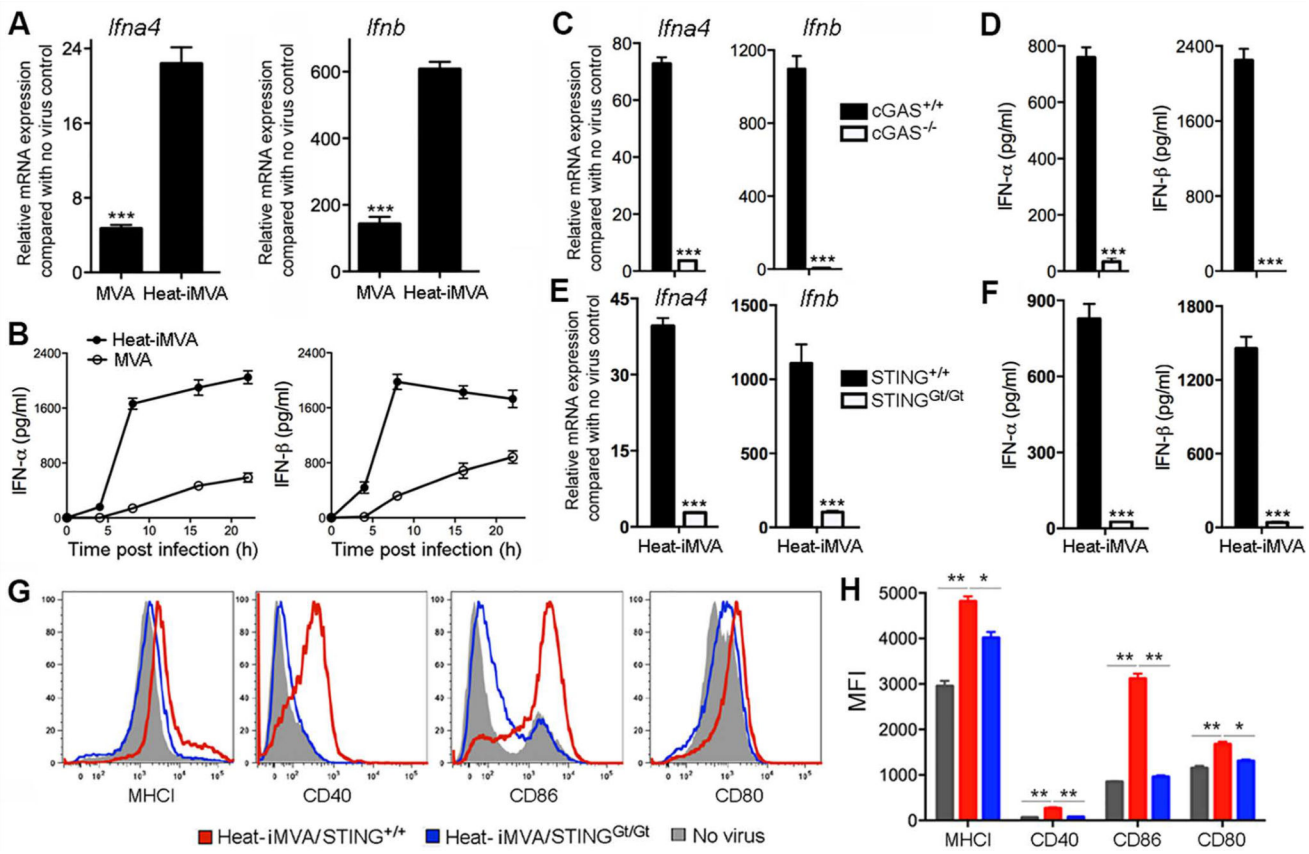

Fig. 1. Heat-iMVA induces higher levels of type I IFN production via the cGAS/STING pathway in murine cDCs than MVA

(**A**) Relative *Ifna4* and *Ifnb* mRNA expression levels compared to no virus control in cDCs infected with MVA or with Heat-iMVA. Data are means ± SEM (n=3). A representative experiment is shown, repeated at least twice. (**B**) The concentrations of secreted IFN-α and IFN-β in the medium over time following MVA or Heat-iMVA infection of cDCs (n=3, ***$P < 0.001$, *t* test). (**C**) *Ifna4* and *Ifnb* relative mRNA expression compared with no virus control in cDCs generated from cGAS$^{+/+}$ and cGAS$^{-/-}$ mice and infected with Heat-iMVA (n=3, ***$P < 0.001$, *t* test). (**D**) Concentrations of secreted IFN-α and IFN-β in the medium of cDCs generated from cGAS$^{+/+}$ and cGAS$^{-/-}$ mice and infected with Heat-iMVA (n=3, ***$P < 0.001$, *t* test). (**E**) *Ifna4* and *Ifnb* relative mRNA expression compared with no virus control in cDCs generated from STING$^{+/+}$ and STING$^{Gt/Gt}$ mice and infected with Heat-iMVA (n=3, ***$P < 0.001$, *t* test). (**F**) Concentrations of secreted IFN-α and IFN-β in the medium of cDCs generated from STING$^{+/+}$ and STING$^{Gt/Gt}$ mice and infected with Heat-iMVA (n=3, ***$P < 0.001$, *t* test). (**G, H**) Representative flow cytometry data (G) and MFI (H) of expression of surface markers MHCI (MHC class I), CD40, CD86, and CD80 in Heat-iMVA infected cDCs generated from STING$^{Gt/Gt}$ and WT mice (n=3, *$P < 0.05$, **$P < 0.01$, *t* test).

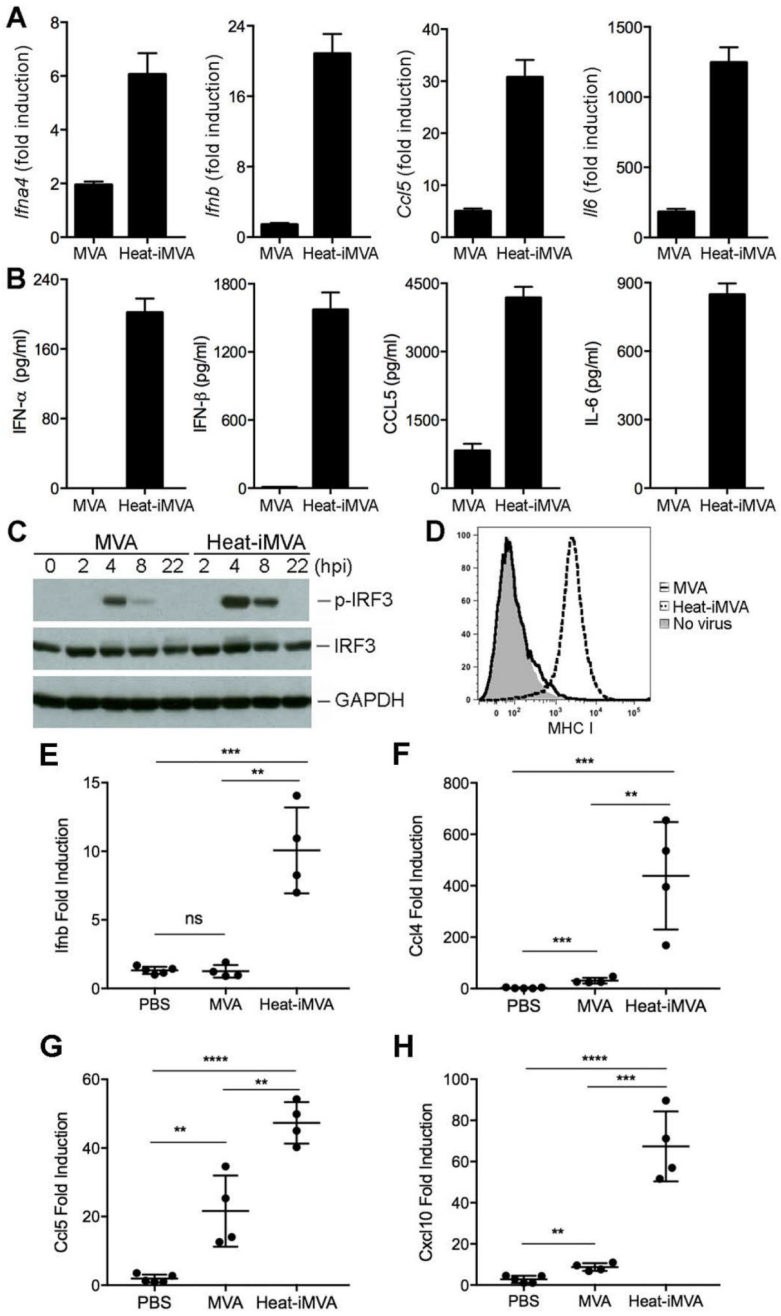

Fig. 2. Heat-iMVA infection of B16-F10 melanoma cells induces type I IFN, proinflammatory cytokines and chemokines in vitro and in vivo

(**A**) The relative mRNA expression of *Ifna4, Ifnb, Ccl5*, and *Il6* in B16-F10 cells infected with either MVA or Heat-iMVA. Data are means ± SEM (n=3). (**B**) Concentrations of secreted IFN-α, IFN-β, CCL5, and IL-6 in the medium of B16-F10 cells infected with either MVA or Heat-iMVA. (**C**) Western Blot showing protein levels of p-IRF-3, IRF3, and GAPDH. "hpi", hours post infection. (**D**) Expression of surface markers MHCI (MHC class I) in B16-F10 cells infected with either MVA, Heat-iMVA or mock infection control. Representative experiments are shown, repeated once. (**E-H**) quantitative real-time PCR

analyses of *Ifnb, Ccl4, Ccl5*, and *Cxcl10* gene expression in injected B16-F10 tumors treated with either PBS, MVA or Heat-MVA (n=4–5, $^{**}P < 0.01$, $^{***}P < 0.001$, $^{****}P < 0.0001$, *t* test).

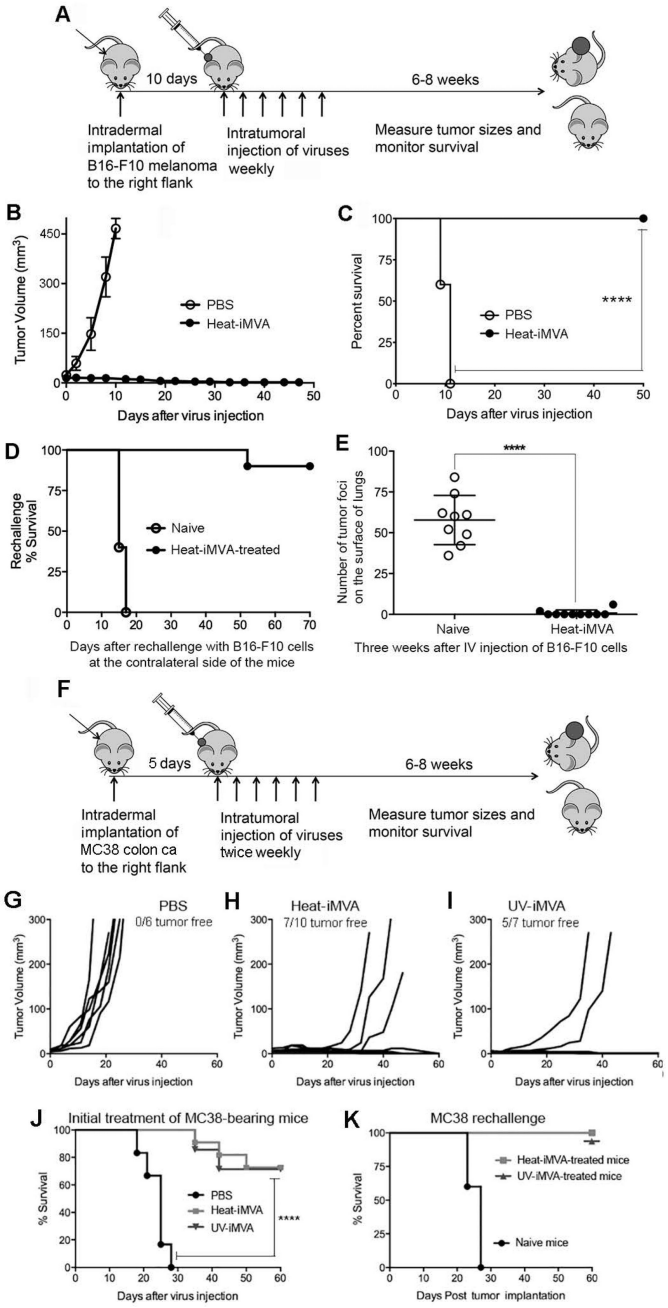

Fig. 3. Intratumoral injection Heat-iMVA eradicates B16-F10 melanoma and MC38 colon adenocarcinoma and induces systemic antitumor immunity

(**A**) Tumor implantation and treatment scheme for a B16-F10 unilateral tumor implantation model. (**B**) Tumor volume against time (days) after PBS (n=5) or Heat-iMVA (n=10) injection. A representative experiment is shown, repeated at least three times. (**C**) Kaplan-Meier survival curve of tumor-bearing mice injected with PBS (n=5) or Heat-iMVA (n=10) (**** $P < 0.0001$, Mantel-Cox test). A representative experiment is shown, repeated at least three times. (**D**) Kaplan-Meier survival curve of naïve mice (n=5) and Heat-iMVA-treated mice (n=10) re-challenged at the contralateral side with a lethal dose of B16-F10 melanoma

cells (1×10^5 cells). A representative experiment is shown, repeated at least three times. (E) The number of tumor foci on the surface of lungs collected at 3 weeks from either naïve mice (n=9) or Heat-iMVA-treated mice (n=10) after intravenous delivery of 1×10^5 cells (****$P < 0.0001$, *t* test). (F) Tumor implantation and treatment scheme for a MC38 unilateral tumor implantation model. 1×10^5 MC38 colon adenocarcinoma cells were implanted intradermally on the right flank of shaved mice. After 7 days, tumors were injected with either PBS, Heat-MVA, or UV-MVA (inactivated equivalent of 2×10^7 pfu) twice weekly. Tumor volumes plotted against days after various treatment regimens including PBS (**G**, n=6), Heat-iMVA (**H**, n=10), UV-iMVA (**I**, n=7). (**J**) Kaplan-Meier survival curve of mice treated with either PBS, Heat-iMVA, or UV-iMVA (****P < 0.0001, Mantel-Cox test). (**K**) Kaplan-Meier survival curve of naïve mice (n=5), Heat-iMVA-treated mice (n=7), UV-iMVA-treated mice (n=5) re-challenged at the contralateral side with a lethal dose of MC38 cells (1×10^5 cells). A representative experiment is shown, repeated once.

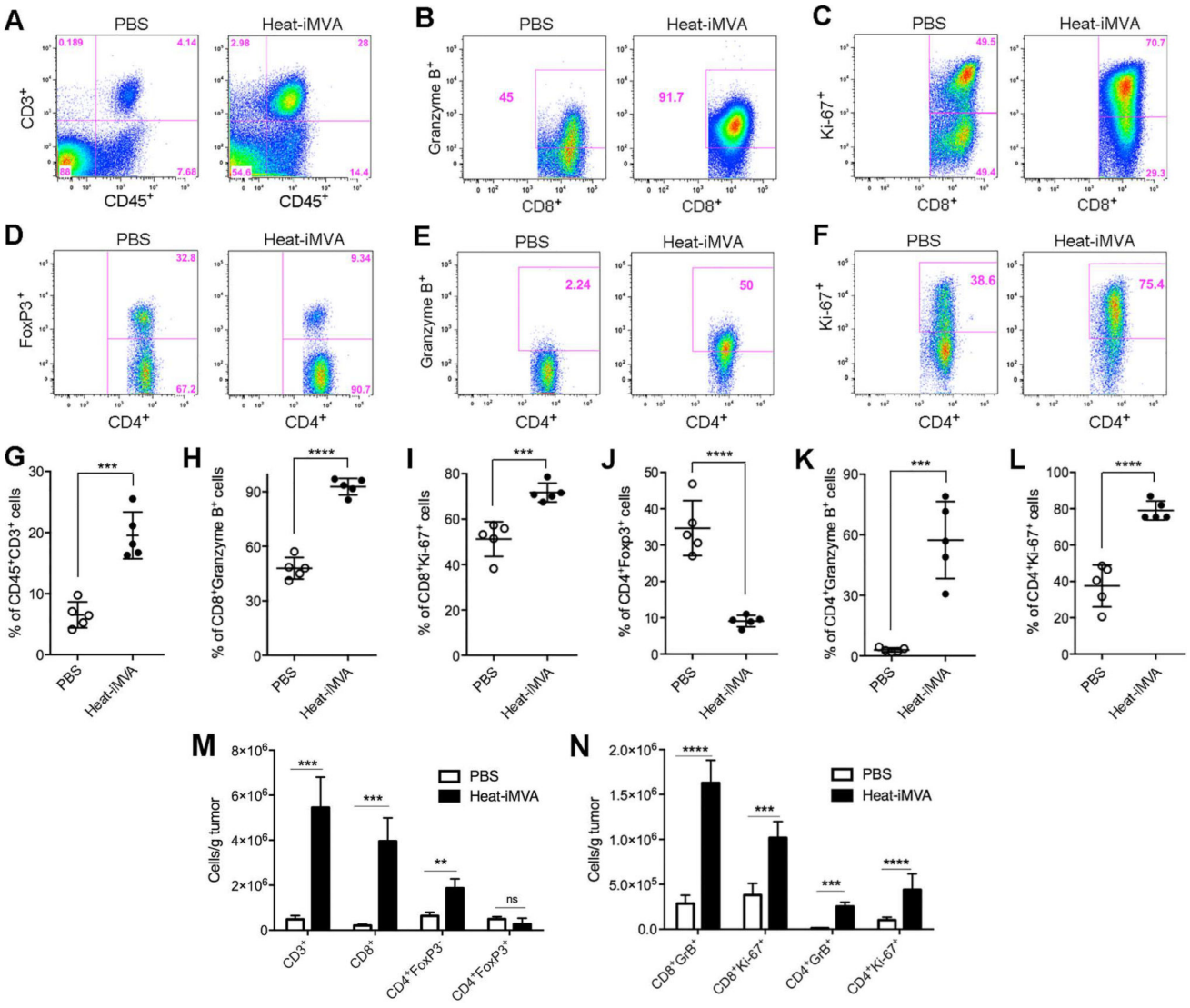

Fig. 4. Intratumoral injection of Heat-iMVA leads to immunological changes in the tumor microenvironment

5×10^5 B16-F10 melanoma cells were implanted intradermally to the right flank of the mice. Seven days post implantation, we injected either Heat-iMVA (an equivalent of 2×10^7 pfu) or PBS into the tumors on the right flank. The injection was repeated three days later. Tumors were harvested 3 days post last injection and cell suspensions were generated. The live immune cell infiltrates in the tumors were analyzed by FACS. (**A-F**) Representative flow cytometry plot of $CD3^+$ $CD45^+$ T cells (**A**), $CD8^+$ cells expressing Granzyme B^+ (**B**) or Ki-67 (**C**), $CD4^+$ cells expressing FoxP3 (**D**), Granzyme B (**E**), or Ki-67 (**F**). (**G-L**) Percentages of $CD45^+$ $CD3^+$ (**G**), $CD8^+$ Granzyme B^+ (**H**), $CD8^+$ Ki-67$^+$ (**I**), $CD4^+$ Foxp3$^+$ (**J**), $CD4^+$ Granzyme B^+ (**K**), and $CD4^+$ Ki67$^+$ (**L**) cells within tumors of mice treated with PBS (n=5) or Heat-iMVA (n=5; ***$P < 0.001$; ****$P < 0.0001$, *t* test). A representative experiment is shown, repeated at least twice. (**M**) The absolute numbers of tumor infiltrating $CD3^+$, $CD8^+$, $CD4^+$ FoxP3$^-$, and $CD4^+$ FoxP3$^+$ cells per gram of injected tumors treated with either Heat-iMVA or PBS (n=5; **$P < 0.01$; ***$P < 0.001$, *t* test). (**N**) The absolute

numbers of $CD8^+$ Granzyme B^+, $CD8^+$ $Ki67^+$, $CD4^+$ Granzyme B^+, and $CD4^+$ $Ki67^+$ cells in the injected tumors treated with either Heat-iMVA or PBS (n=5; ***$P < 0.001$; ****$P < 0.0001$, *t* test).

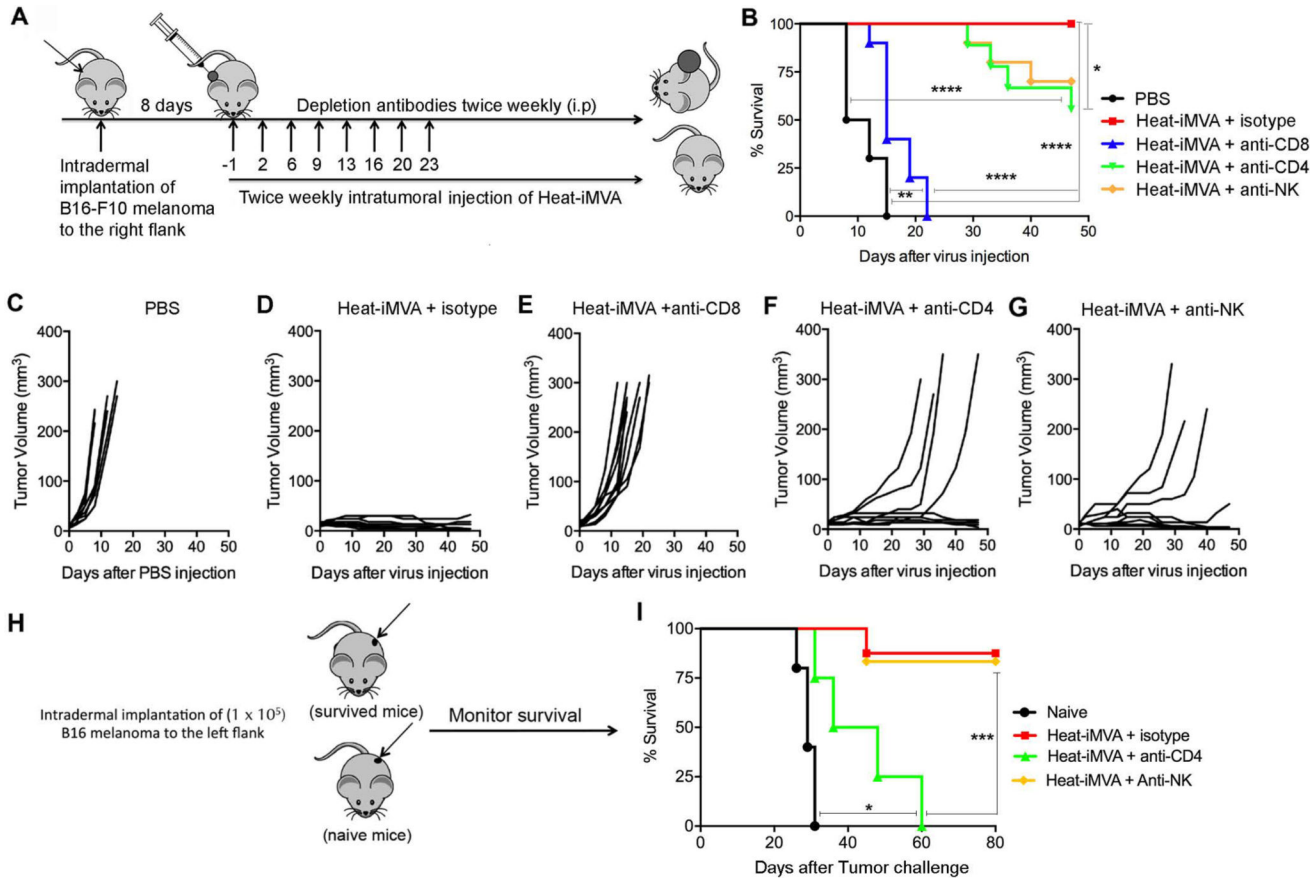

Fig. 5. CD8$^+$ T cells are critical for Heat-iMVA-induced antitumor effect and CD4$^+$ T cells contribute to the development of systemic immunity against tumor re-challenge

(**A**) Schematic diagram of intratumoral injection of Heat-iMVA in the presence or absence of depleting antibodies for CD4$^+$, CD8$^+$, and NK cells in a unilateral B16-F10 melanoma implantation model. (**B**) Kaplan-Meier survival curve of mice treated with either PBS or Heat-iMVA in the presence of isotype control, CD4$^+$, CD8$^+$, and NK cells-depleting antibodies (n=10; *$P < 0.05$; **$P < 0.01$; ****$P < 0.0001$, Mantel-Cox test). (**C-G**) Tumor volumes plotted against days after various treatment regimens including PBS (**C**), Heat-iMVA+control (**D**), Heat-iMVA+anti-CD8 (**E**), Heat-iMVA+anti-CD4 (**F**), and Heat-iMVA +anti-NK (**G**). (**H**) Schematic diagram of tumor re-challenge with intradermal implantation of a lethal dose of B16-F10 cells at the left flank in naïve mice and surviving mice treated with Heat-iMVA for the original tumor implanted at the right flank in the presence or absence of CD4$^+$ and NK cell depletion. (**I**) Kaplan-Meier survival curve of naïve mice (n=6), Heat-iMVA-treated mice (n=10), Heat-iMVA-treated mice with NK depletion (n=6), and Heat-iMVA-treated mice with CD4$^+$ T cell depletion (n=6), re-challenged at the contralateral side with a lethal dose of B16-F10 melanoma cell re-challenge (*$P < 0.05$; ***$P < 0.001$; Mantel-Cox test).

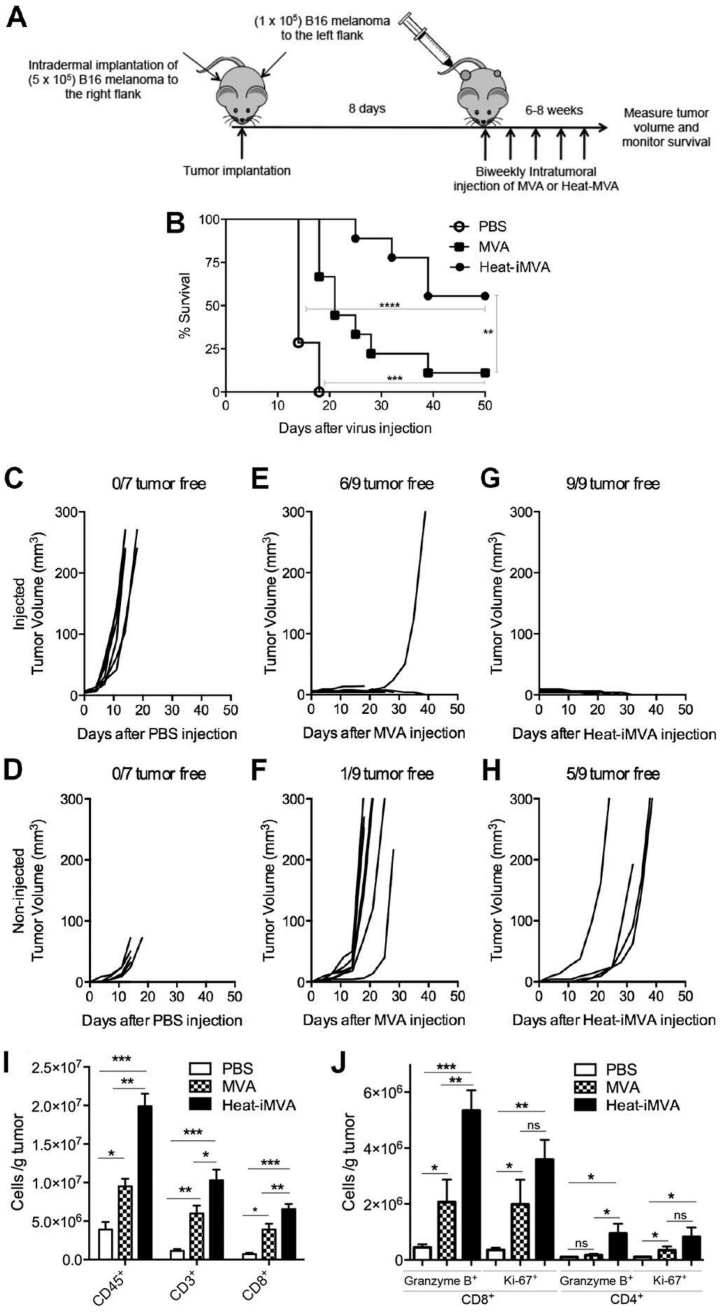

Fig. 6. Intratumoral injection of Heat-iMVA is more effective than MVA in eradicating the injected tumors as well as controlling the growth of non-injected tumors

(**A**) Scheme of treatment plan in which B16-F10 melanomas were treated with either MVA or Heat-MVA intratumorally in a bilateral intradermal tumor implantation model. (**B**) Kaplan-Meier survival curve of tumor-bearing mice treated either PBS, MVA, or Heat-MVA (n=7 or 9, $^{**}P < 0.01$; $^{***}P < 0.001$; Mantel-Cox test). (**C-D**) Volumes of injected (**C**) and non-injected (**D**) tumors over days after PBS injection. (**E-F**) Volumes of injected (**E**) and non-injected (**F**) tumors over days after MVA injection. (**G-H**) Volumes of injected (**G**) and non-injected (**H**) tumors over days after Heat-MVA injection. A representative experiment is

shown, repeated twice. (**I**) Absolute numbers of tumor infiltrating $CD45^+$, $CD3^+$, and $CD8^+$ per gram of non-injected tumors after intratumoral injection of PBS (n=5), MVA (n=5) or Heat-iMVA (n=5) to the contralateral tumors. (**J**) Absolute numbers of tumor infiltrating Granzyme B^+ $CD8^+$, $Ki67^+$ $CD8^+$, Granzyme B^+ $CD4^+$, and $Ki67^+$ $CD4^+$ cells per gram of non-injected tumors after intratumoral injection of PBS, MVA, or Heat-iMVA to the contralateral tumors. Data are means ± SEM (n=5, $*P < 0.05$; $**P < 0.01$; $***P < 0.001$; *t* test). A representative experiment is shown, repeated once.

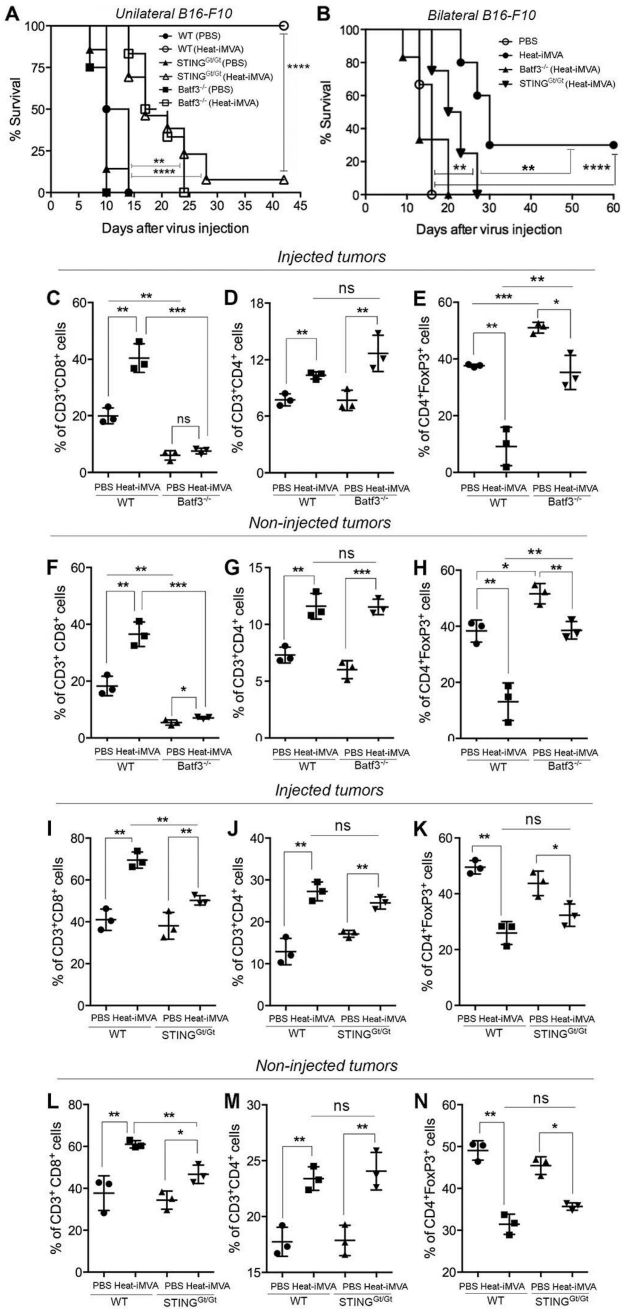

Fig. 7. Heat-iMVA is less effective in eradicating B16-F10 melanomas in STING-deficient mice or Batf3-deficient mice compared with wild-type controls

(**A**) Kaplan-Meier survival curve of WT, STING$^{Gt/Gt}$, and Batf3$^{-/-}$ mice with unilateral implantation of B16-F10 melanoma and treated with PBS or Heat-iMVA (n=5–8; $^{**}P < 0.01$; $^{****}P < 0.0001$; Mantel-Cox test). A representative experiment is shown, repeated once. (**B**) Kaplan-Meier survival curve of WT, STING$^{Gt/Gt}$, and Batf3$^{-/-}$ mice with bilateral implantation of B16-F10 melanoma and treated with PBS or Heat-iMVA to the larger tumors on the right flank (n=6–8; $^{**}P < 0.01$; $^{****}P < 0.0001$; Mantel-Cox test). A representative experiment is shown, repeated once. (**C, D**) the absolute numbers of CD3$^+$, CD8$^+$, CD4$^+$ FoxP3$^-$, CD4$^+$ FoxP3$^+$ cells and the ratios of CD8$^+$/Treg and CD4$^+$ FoxP3$^-$

(Tconv)/CD4$^+$ FoxP3$^+$ (Treg) in the injected (**C**) or non-injected (**D**) tumors from PBS or Heat-iMVA-treated WT or Batf3$^{-/-}$ mice. (**E, F**) the absolute numbers of CD3$^+$, CD8$^+$, CD4$^+$ FoxP3$^-$, CD4$^+$ FoxP3$^+$ cells and the ratios of CD8$^+$/Treg and CD4$^+$ FoxP3$^-$ (Tconv)/CD4$^+$ FoxP3$^+$ (Treg) in the injected (**E**) or non-injected (**F**) tumors from PBS or Heat-iMVA-treated WT or STING$^{Gt/Gt}$ mice. (n=3; *$P < 0.05$, **$P < 0.01$, ***$P < 0.001$; ns, nonsignificant; *t* test). A representative experiment is shown, repeated once.

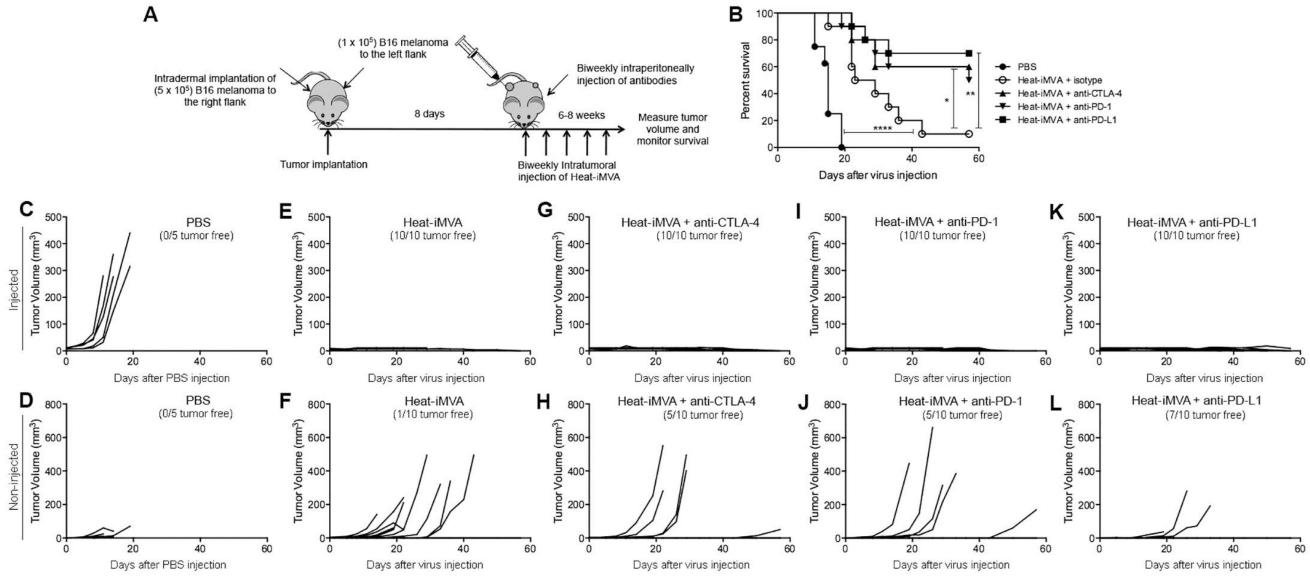

Fig. 8. The combination of intratumoral injection of Heat-iMVA with systemic delivery of anti-CTLA-4, anti-PD-1, or anti-PD-L1 antibodies significantly increases the overall response and cure rates in a B16-F10 bilateral implantation model

(**A**) Scheme of treatment plan in which B16-F10 melanomas were treated with either intratumoral delivery of PBS or Heat-iMVA with or without systemic delivery of immune checkpoint blockade antibodies in a bilateral intradermal tumor implantation model. (**B**) Kaplan-Meier survival curve of tumor-bearing mice treated with PBS, Heat-MVA + isotype control, Heat-MVA + anti-CTLA4 antibody, Heat-MVA + anti-PD1 antibody, or Heat-MVA + anti-PD-L1 antibody (n=5 or 10; $*P < 0.05$; $**P < 0.01$; $****P < 0.0001$; Mantel-Cox test). (**C-L**) Volumes of injected (**C**) and non-injected (**D**) tumor over days after PBS injection, after intratumoral injection of Heat-MVA and intraperitoneal delivery of isotype control (**E, F**), after intratumoral injection of Heat-MVA and intraperitoneal delivery of anti-CTLA-4 antibody (**G, H**), after intratumoral injection of Heat-MVA and intraperitoneal delivery of anti-PD-1 antibody (**I, J**), after intratumoral injection of Heat-MVA and intraperitoneal delivery of anti-PD-L1 antibody (**K, L**). A representative experiment is shown, repeated twice.